学位論文
Doctor's Thesis

Id1 Gene Transfer Confers Angiogenic Property on Fully Differentiated Endothelial Cells and Contributes to Therapeutic Angiogenesis

(Id1 遺伝子導入成熟内皮細胞は血管新生能が亢進し治療的血管新生に寄与する)

西山　功一

Koichi Nishiyama

熊本大学大学院医学研究科博士課程内科系専攻循環器内科学

指導：小川　久雄　教授

2005 年度

Contents

I. Abstract

Transplantation of endothelial progenitor cells has been proposed as a potential strategy for therapeutic revascularization. However, the limited endogenous cell pool and the related technical difficulties constitute clinically important disadvantages to autologous transplantation. In this study, we investigated whether fully differentiated endothelial cells (ECs) modified with gene transfer of inhibitor of differentiation-1 (Id1), a helix-loop-helix transcription factor involved in angiogenesis, have the potential to contribute to therapeutic angiogenesis. The Id1 gene was transferred into human umbilical vein ECs (HUVECs) via a Sendai virus vector. Id1 stimulated migration, proliferation and capillary-like tube/cord formation of HUVECs. In addition, Id1 reduced serum deprivation-induced HUVEC apoptosis as shown by fluorescence activated cell sorting (FACS) analysis with annexin V and terminal deoxynucleotidyl transferase mediated biotin nick end-labeling (TUNEL) staining. Transplantation of Id1-overexpressing HUVECs accelerated recovery of blood-flow as evaluated by Laser Doppler perfusion imaging, increased capillary density, and improved the rate of limb salvage, as compared to the transplantation of control HUVECs. Histochemical analysis revealed that the regenerated vascular networks of limbs transplanted with Id1-overexpressing HUVECs contained numerous HUVECs, some of which were in a proliferative state. Untransfected HUVECs were also incorporated with Id1-transfected HUVECs, suggesting the non-cell autonomous effect of Id1. Finally, angiopoietin-1 was upregulated in Id1-overexpressing HUVECs and functionally contributed to the *in vitro* angiogenic effect of Id1. Id1 gene transfer conferred HUVECs with an angiogenic property, contributing to neovascularization after transplantation into ischemic lesions. Transplantation of Id1-overexpressing mature ECs may serve as a novel and useful strategy for therapeutic angiogenesis.

II. The List of Publication

1. Nishiyama K, Takaji K, Kataoka K, Kurihara Y, Yoshimura M, Kato K, Ogawa H, Kurihara H.
Id1 gene transfer confers angiogenic property on fully differentiated endothelial cells and contributes to therapeutic angiogenesis.
Circulation. 2005;112:2840-50.

2. Kushiyama A, Shojima N, Ogihara T, Inukai K, Sakoda H, Fujishiro M, Fukushima Y, Anai M, Ono H, Horike N, Viana AY, Uchijima Y, Nishiyama K, Shimosawa T, Fujita T, Katagiri H, Oka Y, Kurihara H, Asano T.
Resistin like molecule beta activates MAPKs, suppresses insulin signaling in hepatocytes and induces diabetes, hyperlipidemia and fatty liver in transgenic mice on a high-fat diet.
J Biol Chem. 2005;280(51):42016-25.

3. Nishiyama K, Yasue H, Moriyama Y, Tsunoda R, Ogawa H, Yoshimura M, Kugiyama K.
Acute effects of melatonin administration on cardiovascular autonomic regulation in healthy men.
Am Heart J. 2001;141(5):E9.

4. Ogawa H, Suefuji H, Soejima H, Nishiyama K, Misumi K, Takazoe K, Miyamoto S, Kajiwara I, Sumida H, Sakamoto T, Yoshimura M, Kugiyama K, Yasue H, Matsuo K.
Increased blood vascular endothelial growth factor levels in patients with acute myocardial infarction.
Cardiology. 2000;93(1-2):93-9.

5. Moriyama Y, Yasue H, Yoshimura M, Mizuno Y, Nishiyama K, Tsunoda R, Kawano H, Kugiyama K, Ogawa H, Saito Y, Nakao K.
The plasma levels of dehydroepiandrosterone sulfate are decreased in patients with chronic heart failure in proportion to the severity.
J Clin Endocrinol Metab. 2000;85(5):1834-40.

6. Ogawa H, Sakamoto T, Nishiyama K, Soejima H, Kaikita K, Takazoe K, Miyamoto S, Kugiyama K, Yoshimura M, Yasue H
Elevated levels of soluble intercellular adhesion molecule-1 in the coronary circulation of patients with coronary organic stenosis and spasm.
Jpn Circ J. 2000;64(3):170-6.

7. Soejima H, Ogawa H, Yasue H, Kaikita K, Takazoe K, Nishiyama K, Misumi K, Miyamoto S, Yoshimura M, Kugiyama K, Nakamura S, Tsuji I.
Angiotensin-converting enzyme inhibition reduces monocyte chemoattractant protein-1 and tissue factor levels in patients with myocardial infarction.
J Am Coll Cardiol. 1999;34(4):983-8.

8. Soejima H, Ogawa H, Yasue H, Kaikita K, Nishiyama K, Misumi K, Takazoe K, Miyao Y, Yoshimura M, Kugiyama K, Nakamura S, Tsuji I, Kumeda K.
Heightened tissue factor associated with tissue factor pathway inhibitor and prognosis in patients with unstable angina.
Circulation. 1999;99(22):2908-13.

9. Ogawa H, Yasue H, Miyao Y, Sakamoto T, Soejima H, Nishiyama K, Kaikita K, Suefuji H, Misumi K, Takazoe K, Kugiyama K, Yoshimura M.
Plasma soluble intercellular adhesion molecule-1 levels in coronary circulation in patients with unstable angina.
Am J Cardiol. 1999;83(1):38-42.

10. Soejima H, Ogawa H, Yasue H, Nishiyama K, Kaikita K, Misumi K, Takazoe K, Kugiyama K, Tsuji I, Kumeda K, Nakamura S.
Plasma tissue factor pathway inhibitor and tissue factor antigen levels after administration of heparin in patients with angina pectoris.
Thromb Res. 1999;93(1):17-25.

11. Moriyama Y, Ogawa H, Oshima S, Arai H, Takazoe K, Shimomura H, Hirai N, Suefuji H, Soejima H, Nishiyama K, Misumi K, Yasue H.
Relationship between serum angiotensin-converting enzyme activity and plasma plasminogen activator inhibitor activity in patients with recent myocardial infarction.
Coron Artery Dis. 1998;9(10):691-6.

12. Nishiyama K, Ogawa H, Yasue H, Soejima H, Misumi K, Takazoe K, Yoshimura M, Kugiyama K, Tsuji I, Kumeda K.
Simultaneous elevation of the levels of circulating monocyte chemoattractant protein-1 and tissue factor in acute coronary syndromes.
Jpn Circ J. 1998;62(9):710-2.

13. Misumi K, Ogawa H, Yasue H, Soejima H, Suefuji H, Nishiyama K, Takazoe K, Kugiyama K, Tsuji I, Kumeda K.
Circadian variation in plasma levels of free-form tissue factor pathway inhibitor antigen in patients with coronary spastic angina.
Jpn Circ J. 1998;62(6):419-24.

14. Nishiyama K, Ogawa H, Yasue H, Soejima H, Misumi K, Kugiyama K, Tsuji I, Kumeda K.
Heparin-releasable endothelial cell-associated tissue factor pathway inhibitor (TFPI) is increased in the coronary circulation after coronary spasm in patients with coronary spastic angina.
Thromb Res. 1998;89(3):137-46.

15. Misumi K, Ogawa H, Yasue H, Soejima H, Suefuji H, Nishiyama K, Takazoe K, Kugiyama K, Tsuji I, Kumeda K, Nakamura S.
Comparison of plasma tissue factor levels in unstable and stable angina pectoris.
Am J Cardiol. 1998;81(1):22-6.

16. Soejima H, Ogawa H, Yasue H, Suefuji H, Kaikita K, Nishiyama K.
Effects of imidapril therapy on endogenous fibrinolysis in patients with recent myocardial infarction.
Clin Cardiol. 1997;20(5):441-5.

17. Suefuji H, Ogawa H, Yasue H, Imoto N, Sakamoto T, Miyao Y, Kaikita K, Soejima H, Nishiyama K.
Effect of niceritrol on fibrinolysis and lipoprotein (a) levels in patients with coronary artery disease.
Coron Artery Dis. 1996;7(2):167-72.

18. Saito T, Yashita S, Noda K, Mizuno Y, Kawabata S, Higa T, Nakahashi E, Iwasa A, Nishiyama K, Ohshima S.
Clinical experience with the ACS RX Lifestream coronary dilatation catheter: a new low profile perfusion balloon catheter.
J Invasive Cardiol. 1995;7 Suppl B:39B-45B; discussion 50B-56B.

III. Acknowledgements

I appreciate Dr. Hisao Ogawa, Professor of the Department of Cardiovascular Medicine, Graduate School of Medical Sciences, Kumamoto University for his continuous suggestions and encouragements. I am also grateful to Dr. Hiroki Kurihara, Professor of the Department of Biochemistry and Molecular Biology, the University of Tokyo Graduate School of Medicine for continuous suggestions and helping me in the experiments throughout these studies. I thank Dr. Kentaro Takaji and Dr. Keiichiro Kataoka for helpful discussion and helping me in the experiments, especially *in vitro* ones. I thank Dr. Atsushi Kato and Dr. Yukiko Kurihara for helping me in the preparation of viral vector. I also thank Dr. Michihiro Yoshimura, Associate Professor of the Department of Cardiovascular Medicine, Graduate School of Medical Sciences, Kumamoto University for giving me the chance to work in the basic science and Dr. Suda, Professor of the Department of Cell Differentiation, School of Medicine, Keio University for giving me cDNA of angiopoietin-1.

I would like to thank all members of the Department of Cardiovascular Medicine, Graduate School of Medical Sciences, Kumamoto University and of the Department of Biochemistry and Molecular Biology, the University of Tokyo Graduate School of Medicine.

Finally, I thank my parents Mutsumi and Masako Nishiyama for their long-lasting encouragement and support. I also thank my wife Kimiko, daughters Kanako and Yuko, and son Taisei for continuous encouragement and wholehearted assistance.

November 1, 2005 Koichi Nishiyama

IV. Abbreviation

Ang1: angiopoietin-1

Ang2: angiopoietin-2

AP: alkaline phosphatase

BrdU: 5-bromo2'-deoxyuridine

BS-1: Bandeiraea simplicifolia lectin I

CM: conditioned medium

DFX: deferoxamine

DMEM: Dulbecco's modified Eagle's medium

EBM: endothelial basal medium

ECs: endothelial cells

EPCs: endothelial progenitor cells

FACS: fluorescence activated cell sorting

FCS: fetal calf serum

FGF: fibroblast growth factor

FITC: fluorescein isothiocyanate

HLH: helix-loop-helix

HRP: horseradish peroxidase

HUVEC: human umbilical vein endothelial cell

Id: inhibitor of differentiation

LDPI: laser Doppler perfusion imaging

PI: propidium iodide

RT-PCR: reverse transcription-polymerase chain reaction

SeV: Sendai virus

TUNEL: terminal deoxynucleotidyl transferase mediated biotin nick end-labeling

VEGF: vascular endothelial cell growth

vWF: von-Willebrand factor

V. Introduction

Prominent changes in human lifestyle have recently caused not only an increase in the prevalence of ischemic diseases based on atherosclerosis, but also their disease complexity due to concomitant metabolic disorders. On the other side, progress in mechanical revascularization by catheter and surgical interventions, together with newly developed pharmacological therapeutics, has improved survival rate and quality of life in patients with complex ischemic diseases. However, there remains a significant population of patients who are resistant to current treatment approaches and demand urgent alternatives.

The last decade has seen exceptional scientific progress in the field of vascular biology, which brought a new therapeutic model termed "therapeutic revascularization" [1-4]. One is the identification of angiogenic factors as typified by vascular endothelial cell growth factor (VEGF) and fibroblast growth factor (FGF) families, which predominantly act on pre-existing endothelial cells (ECs) to promote EC proliferation, migration and morphogenetic activity [5, 6]. Based on their effects, angiogenic gene therapy has been tried for therapeutic revascularization.

The other striking progress is derived from the discovery of circulating endothelial progenitor cells (EPCs) [7, 8]. In response to cytokines, EPCs are mobilized from the bone marrow, recruited to the site of wound healing, tissue ischemia and tumor growth, and then differentiated into vascular endothelial cells (ECs) [6-10]. This process, termed "postnatal vasculogenesis", is postulated, together with angiogenesis, to contribute to regional neovascularization [10]. Several animal experiments and human trials under way are focused on the potential application of EPCs to vascular regenerative therapy [11] (Figure 1).

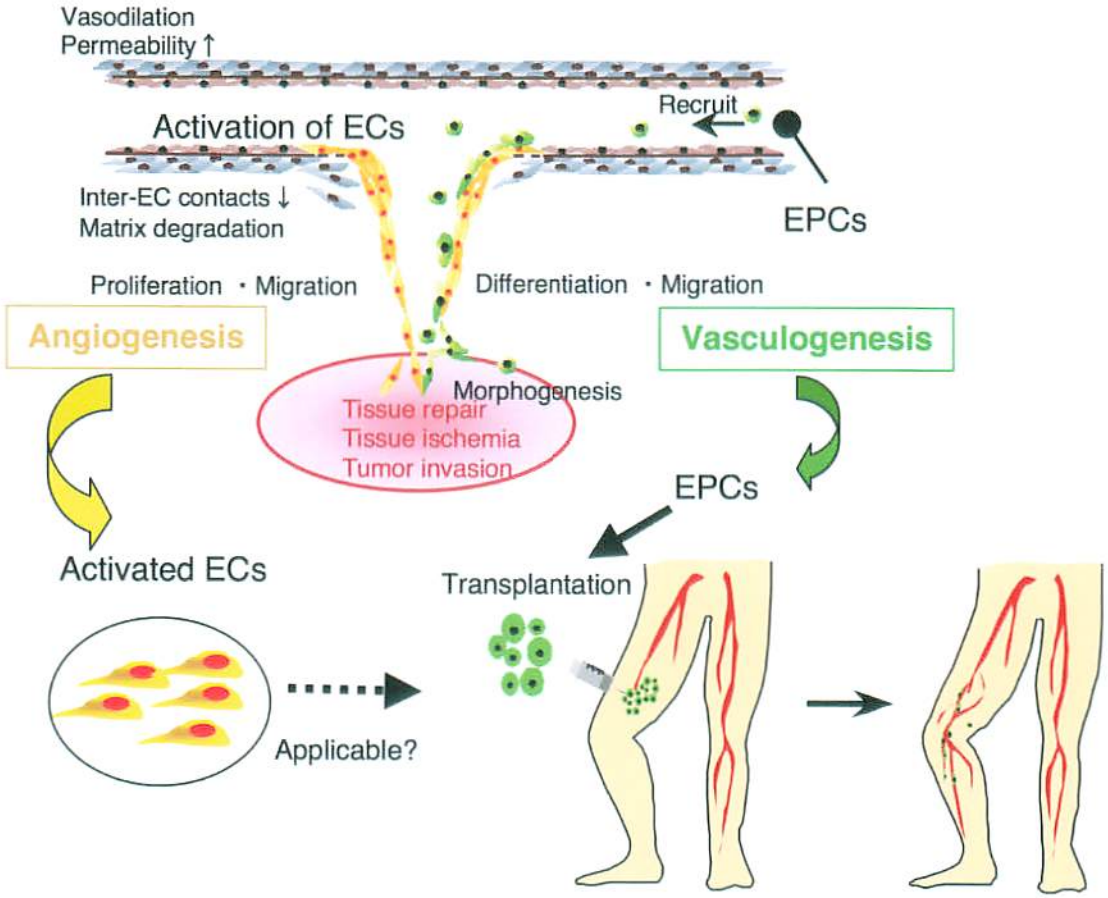

Figure 1. A conceptual diagram of physiological, pathological and therapeutic revascularization. One important angiogenic process is termed as "angiogenesis", in which pre-existing ECs are activated, proliferate and migrate to form new blood vessels. The other important one is termed "postnatal vasculogenesis", in which EPCs are recruited into focal regenerative lesion, and then differentiate into ECs to form new blood vessels. Nowadays, interest in vascular regenerative therapy is focused on cell therapy with EPCs based on the mechanistic understanding of vasculogenesis.

Cell therapy with EPCs and ECs may be more advantageous than gene therapy for vascular regenerative therapy. First, EPCs or ECs vigorously express many kinds of growth factors, and thus transplanted cells themselves can be important sources of the factors. Secondly, regardless of how much growth factor is administered, the resident population of ECs that is competent to respond to administered growth factor is often limited [4]. Therefore, it would require the supply of EPCs or ECs from other sources to regenerate vasculature in an effective way.

Although the usefulness of EPCs for therapeutic revascularization is highly anticipated, several issues remain unresolved. Most notably, the limited cell pool and technical difficulties in expanding EPCs *in vitro* have prevented widespread clinical use of EPCs for autologous transplantation. Differentiated vascular ECs, on the other hand, can be isolated and expanded *in vitro* [12, 13]. Moreover, a large number of mature ECs can be differentiated from bone marrow-derived progenitor cells and embryonic stem cells [14, 15] as shown in Figure 2. Thus, it would be advantageous for mature ECs to serve as a cell source for neovascularization. However, mature ECs are inefficiently incorporated into forming vessels, such that their contribution to therapeutic angiogenesis is limited [16]. The fact that ECs in adult organs transform phenotypically into "angiogenic" cells under pathological circumstances and participate in neovascularization [6] prompted me to hypothesize that quiescent ECs may become "angiogenic" via phenotypic modification with gene transfer and so on.

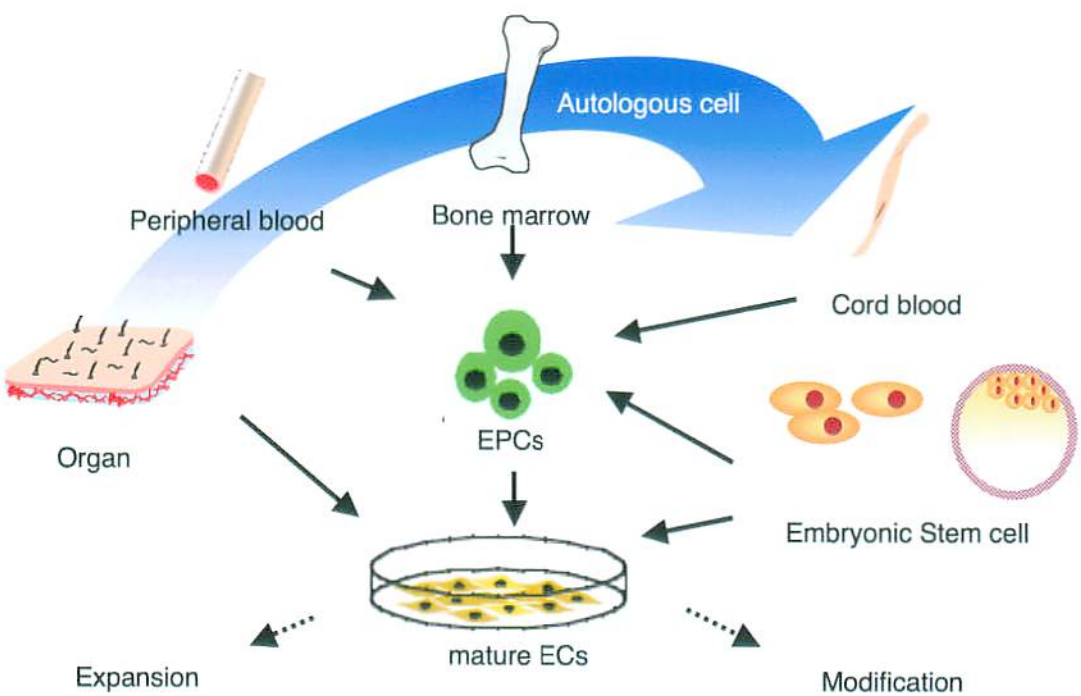

Figure 2. Potential sources of ECs. Differentiated vascular ECs can be isolated and expanded *in vitro*. Moreover, a number of mature ECs can be differentiated from a variety of cell source, mostly autologous cell sources.

The inhibitor of differentiation (Id) proteins (four known members called Id1, Id2, Id3, and Id4 in vertebrates; 13-20kDa) are a family of helix-loop-helix (HLH) transcription factors [17]. Four main groups of HLH protein can be distinguished on the basis of the presence or absence of additional functional domains (Figure 3). The highly conserved HLH region comprises two amphipathic α helices, each 15-20 residues long, which are separated by a shorter intervening loop that has a more variable length and sequence [18]. The HLH domain primarily mediates homo- or hetero-dimerization, which is essential for DNA binding and transcriptional regulation [18]. Nearly all HLH proteins possess a region of highly basic residues adjacent to the HLH domains, which facilitates binding to DNA containing the canonical 'E Box' recognition sequence, CANNTG [18] (Figure 3). Id proteins lack a basic DNA binding domain and primarily act as inhibitors of basic HLH transcription factors, via hetero-dimerization [17] (Figure 3). Through this mechanism, Id proteins have been implicated in regulating a variety of cellular processes including cell growth, senescence, differentiation, and neoplastic transformation [17, 19, 20].

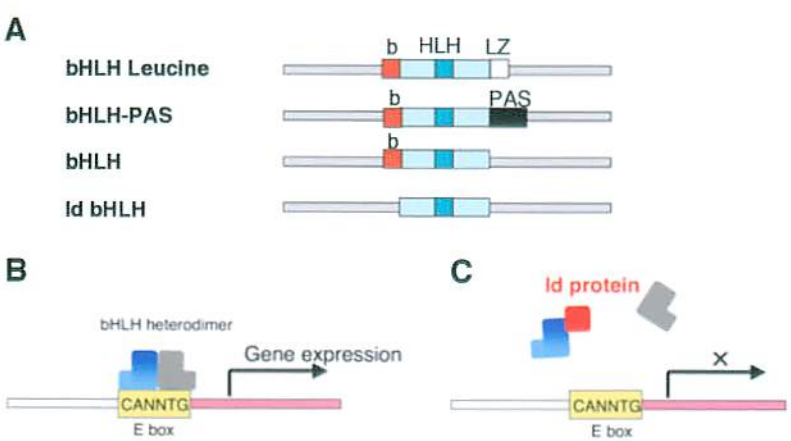

Figure 3. Transcriptional control of tissue specific genes by Id proteins. A, Schematic structure of different HLH protein families. The basic DNA-binding region (b), leucine zipper (LZ) and PAS domains that bound the HLH region are shown. B, C, The ubiquitously expressed basic HLH E protein transcriptional factors activate transcription by binding to promoter E boxes as E protein and E protein homodimers or as E protein-tissue specific basic HLH factor heterodimers (B). Formation of Id protein-E protein dimers prevents E proteins from forming DNA-binding transcriptionally active complexes (C).

More recently, accumulating evidence has suggested that Id1 and Id3 play vital roles in regulating angiogenesis during embryonic development and tumorigenesis [21-23]. Id1/Id3 double knockout embryos display vascular malformations in the forebrain, leading to fatal hemorrhage [21]. Partial Id1 and Id3 deficiencies impaired tumor angiogenesis in tumor-transplanted [21, 22] and spontaneously tumorigenic murine models [23, 24]. Id1 and Id3 are highly expressed in tumor vasculature ECs in comparison to ECs from normal tissue [23]. Furthermore, ectopic expression of Id1 on cultured ECs enhanced capillary-like tube formation, reflecting angiogenesis *in vitro* [25]. Therefore, I speculated that transplantation of mature ECs, modified with Id1 gene transfer, would enhance neovascularization. To test this hypothesis, I examined whether Id1-transfected human umbilical vein ECs (HUVECs) improved the rate of limb salvage in a mouse model of hindlimb ischemia. For this purpose, we used a mononegavirus vector based on the Sendai virus (SeV), which achieved highly efficient gene transfer into HUVECs. The present results demonstrate that Id1 gene transfer conferred angiogenic properties on HUVECs *in vitro* and *in vivo*. Strikingly, transplantation of Id1-transfected HUVECs rescued ischemic limbs from auto-amputation in athymic nude mice.

VI. Materials and Methods

Antibodies

Polyclonal rabbit anti-SeV antibody was described previously [26]. Rabbit anti-Id1 and goat anti-angiopoietin-1 (Ang1) antibodies were purchased form Santa Cruz Biotechnologies. Mouse anti-human CD31 and rat anti-mouse CD31 antibodies were from PharMingen. mouse anti-human Ki67 antibodies from Zymed, mouse anti-β-actin antibody from Sigma, rabbit anti von-Willebrand factor (vWF) antibody and biotinylated and horseradish peroxidase (HRP)-conjugated antibodies against goat immunoglobulins from DAKO, and rhodamine- and HRP-conjugated antibodies against rabbit immunoglobulins and HRP-conjugated antibody against mouse immunoglobulins from Biosource.

Preparation of SeV Vector

The mouse Id1 cDNA was cloned by reverse transcription-polymerase chain reaction (RT-PCR) from total RNA from mouse E10.5 embryos using the following primers:

5'AAgcggccgcCGTACGCCGTAGTAAGAAAAACTTAGGGTGAAAGTTCTCAG GATCATGAAGGTCGCCAG/TTgcggccgcGACGTCCGCCTCAGCGACACAAGA TGCGATC3'. Underlined portions indicate a set of SeV E and S signals connected to the conserved intergenic trinucleotide; the lower case letters represent *Not*I restriction sites. Similarly, the mouse Ang1 cDNA, kindly gifted from Dr. Suda, was amplified using the following primers:

5'AAgcggccgcCGTACGCCGTAGTAAGAAAAACTTAGGGTGAAAGGGCAGTA CAATGACAGTTTTCCTTT/TTgcggccgcGACGTCGCACCTTCAAAAGTCCAAG

GGCCGG3'. The fragments amplified with these primers were purified, digested with *Not*I, and introduced into the *Not*I site of pSeV18c(+) [27]. Then, viruses were recovered using LLCMK2 cells and hen eggs according to previously described procedures [27]. Viral titers were determined using a standard chicken red blood cell hemagglutination assay and a plaque assay on CV1 cells. The process of production of SeV vectors was summarized in Figure 4.

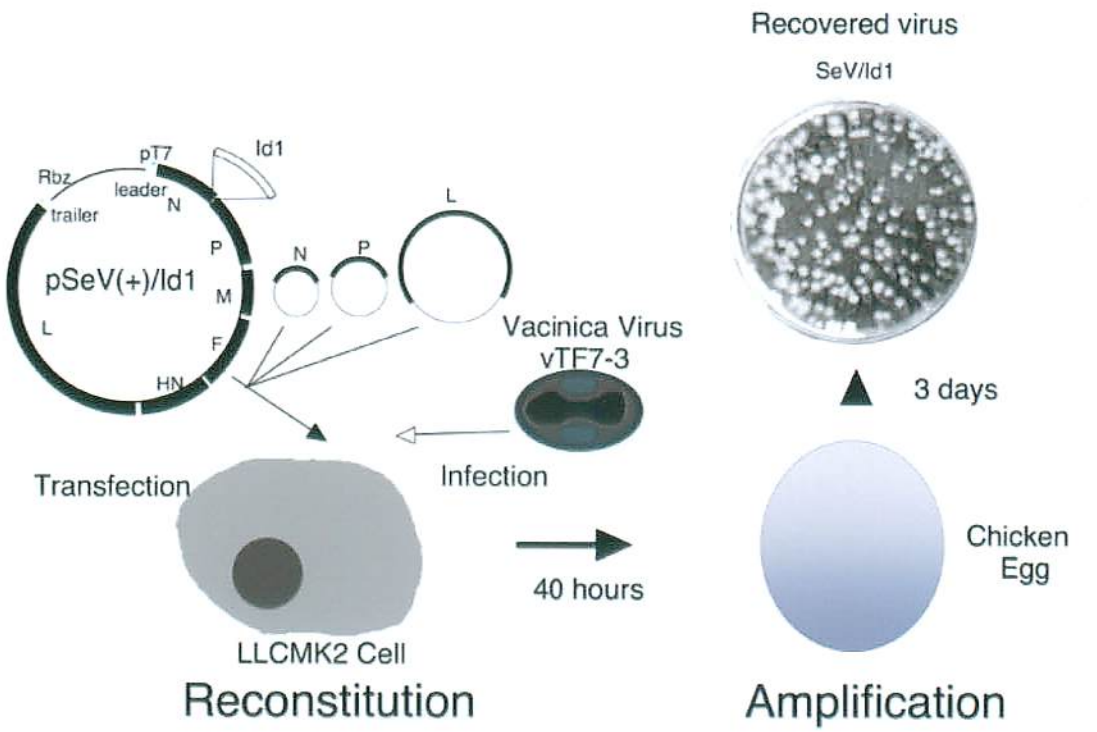

Figure 4. Production of SeV vectors. The Id1 or Ang1 gene was inserted into the downstream region of the N open reading frame of plasmid pSeV18c(+). The resultant plasmid was then used to recover the recombinant SeV in LLCMK2 cells, following the amplification in Chicken eggs. In the recombinant virus, N mRNA transcription is started by its own S signal and is terminated by the synthetic E signal within the inserted Ang1 sequence. N, P, M, F, HN, and L indicate six genes of the SeV genome, encoding nucleocapsid, phospho-, matrix, fusion, hemagglutinin-neuraminidase, and large proteins, respectively.

Cell Culture, Serum Starvation, and Gene Transfer

HUVECs were purchased from Clonetics and maintained in endothelial basal medium (EBM, Clonetics, Inc.) according to the supplier's instructions. COS7 cells were maintained with Dulbecco's modified Eagle's medium (DMEM) containing

10% fetal calf serum (FCS). HUVECs (3 passages) or COS7 cells were transfected with 5-10 multiplicities of infection of recombinant SeV encoding murine Id1 (SeV/Id1), recombinant SeV encoding murine Ang1 (SeV/Ang1), or the control empty vector (SeV/Null). After 1 hour, the viruses were removed by 3 times washing with medium-199, and the cells were cultured for 48 hours in complete medium before each experiment. To determine the best *in vitro* experimental condition, I examined influences of serum stimulation on endogenous Id1 expression in HUVECs. For this purpose, complete medium was replaced with fresh medium-199 with or without 0.5% FCS, 5% FCS, and 10% FCS after extensive washing, and the samples for analysis of Id1 expression were obtained from the cultured HUVECs 0, 1, and 6 hours after the further incubation. On the basis of the results, I decided to perform further experiments after 6 hours' serum starvation with 0.5% FCS-contained medium-199. For analyses of major angiogenic factors and receptors and for the production of conditioned medium, HUVECs or COS7 cells transfected with SeV were recovered in complete medium for 24 hours, after which the medium was substituted with fresh medium-199 with or without 0.5% FCS and the cells were incubated for 24 hours before the assays. HUVECs transfected with SeV were dissociated from culture dishes using appropriate volumes of Hanks'-based cell dissociation buffer (Invitrogen). The conditioned medium (CM) was collected, centrifuged and used for each assay.

RT-PCR

Gene expression was evaluated by semi-quantitative RT-PCR analysis. Total RNA was extracted using Isogen (Nippon gene) and aliquots (1 μg) were then reverse-transcribed using Superscript II (Life Technologies) with random hexamer

primers. The resultant cDNAs were amplified with *Taq* polymerase (Takara) in a thermocycler. Sequences of specific primers used were listed in Table 1. Thermal cycling was performed for 25-30 cycles to maintain PCR conditions within the linear range of amplification before reaching saturation. Each cycle consisted of 30 seconds of denaturation at 94 C°, 1 minute of annealing at each annealing temperature (54 C° for TIE2, 60 C° for Ang1 and Ang2, and 64 C° for Id1, VEGF, Flk-1, Flt-1 and GAPDH), and 1 minute of extension at 72 C°.

Table 1. The list of primers used in the present study.

Gene	Primer	Product
SeV-derived murine Id1	5'CCAGTGGCAGTGCCGCAGCCGCTGCA/ GCGACGTCCGCCTCAGCGACACAA 3'	449-bp
VEGF [28]	5'TTCTGTATCAGTCTTTCCTGGTGAG/ CGAAGTGGTGAAGTTCATGGATG3'	443-bp (VEGF121) 535-bp (VEGF165) 607-bp (VEGF189)
Angiopoieitn-1 [29]	5'GGTCAGAAGAAAGGAGCAAG/ TGGTAGCCGTGTGGTTCTGA3'	437-bp
Angiopoietin-2 [29]	5'GGATCTGGGGAGAGAGGAAC/ CTCTGCACCGAGTCATCGTA3'	516-bp
Flk-1 (KDR) [7]	5'CAACAAAGTCGGGAGAGGAG/ ATGACGATGGACAAGTAGCC3'	816-bp
Flt1 [30]	5'CGACCTTGGTTGTGGCTGACT/ CCCTTCTGGTTGGTGGCTTTG3'	656-bp
TIE2, [29]	5'GGTTCCTTCATCCATT/ GTCCTTCCCATAAACC3'	275-bp
GAPDH [7]	5'TGAAGGTCGGAGTCAACGGATTTG/ CATGTGGGCCATGAGGTCCACCAC3'	983-bp

Real-Time RT-PCR

Primers and TaqMan probes for human Id1 were designed as previously described [31]. The forward primer was 5'-AGAAACCGCAAGGTGAGCAA- 3' (exon1); the reverse primer was 5'-TCCAACTGAAGGTCCCTGATG-3' (exon1); and the TaqMan probe was 5'-TGGAGATTCTCCAGCACGTCATCGACT-3' (exon1). In addition, primers and the TaqMan probe for human GAPDH were purchased from Applied Biosystems. After DNase I (Qiagen) treatment of total RNA, real-time RT-PCR was performed with an ABI PRISM 7900HT Sequence Detector (Applied Biosystems). RT was carried out for 1 cycle at 50°C for 2 minutes, 60°C for 30 minutes, and 95°C for 5 minutes; the PCR protocol consisted of 40 cycles at 94°C for 15 sec and 60°C for 1 minute. Standard curves were obtained for each gene and transcript values were calculated relative to a dilution series of RNA from HeLa cells known as expressing Id1 constantly. Target quantities were normalized to GAPDH and calibrated using 0h values and defined as a value of 1.0. All quantities were expressed as n-fold relative to the calibrator (0h).

Western Blotting

HUVECs were washed twice with cold PBS and suspended in a cold lysis buffer [25 mM HEPES, pH7.5, 300 mM NaCl, 1.5 mM $MgCl_2$, 0.2 mM EDTA, 1% Triton-X100, 0.5 mM DTT, 20 mM β-glycerophosphate, 0.1% SDS, 0.5% sodium deoxycholate, protease inhibitors (complete, Roche)] for Id1 protein assay or a cold lysis buffer [20 mM HEPES pH7.5, 150mM NaCl, 1 mM EDTA, 0.5% Triton-X100, protease inhibitors (complete, Roche)] for the Ang1 protein assay. Similar quantities of the soluble fractions were separated by SDS-PAGE, transferred onto a polyvinylidene difluoride membrane (Millipore), and immunoblotted with the first

antibody. The membrane was then incubated with HRP-conjugated secondary antibody, and the signals were visualized using ECL plus reagent (Amersham). After detection of Ang1 protein, the β-actin protein levels were assayed using the same membrane.

Immunocytochemistry

HUVECs were fixed in 4% paraformaldehyde or 5% dimethyl-sulfoxide/methanol for 20 minutes at 4°C, permeabilized with 0.2% TritonX-100 for 10 minutes at room temperature and blocked in 2% skim milk/PBS for 20 minutes at room temperature. Cells were then incubated with the appropriate antibody for 1 hour at room temperature or over night at 4°C. After extensive washing with 0.2% TritonX-100/PBS (PBS-T), cells were incubated with the appropriate secondary antibody, and for Ang1 staining the signal was subsequently amplified with an avidin-biotin complex system using a Vectastain ABC kit (Vector). If needed, nuclei were stained with Hoechst 33258, and cells were then examined with a computer-assisted microscope (Olympus). In Matrigel culture, cells were first fixed with 4% formalin for 10 minutes at room temperature, embedded in 3% agarose, then treated with 10% formalin for overnight, followed by 70% ethanol [32]. Paraffin embedded sections were prepared and used for Hematoxylin and Eosin staining.

Deferoxamine Treatment

HUVECs were cultured for 24 hours with complete medium before deferoxamine (DFX) treatment, and then indicated amount of DFX was added into the complete media. After 12 or 24 hours' incubation, total RNA was extracted from HUVECs.

Migration Assay

EC migration was evaluated using scratch wound assays [33]. Confluent HUVECs in pre-traced 24-well culture plates were serum-starved with medium-199 containing 0.5% FCS for 6 hours, after which a portion of the cell monolayer was scraped away with a sterile disposable rubber policeman. The remaining cells were gently washed with medium and incubated for 24 hours in medium-199 containing 0.5% FCS. EC migration from the edge of the injured monolayer was quantified by measuring the area between the wound edges, at a random position, before and after incubation using a computer-assisted microscope (Olympus).

DNA Synthesis Assay

DNA synthesis was evaluated by performing a 5-bromo 2'-deoxyuridine (BrdU) incorporation assay with a commercially available kit (Boehringer Mannheim) according to the supplier's instructions. $5x10^3$ HUVECs were plated onto a 96-well plate and then incubated in complete medium for 24 hours. Next, HUVECs were serum-starved with medium-199 containing 0.5% FCS for 6 hours, after which BrdU was added to the medium, followed by further incubation for 8 hours for labeling of HUVECs with or without 10ng/ml of VEGF (R&D). BrdU incorporation was evaluated by the ELISA method with anti-BrdU antibody, and quantified by measuring absorbance at 405/492 nm with a microplate reader (M-Emax, Molecular Devices).

Apoptosis Assay

Apoptosis was induced in HUVECs by the serum deprivation method as previously described [34]. HUVECs were seeded onto 0.2 % gelatin-precoated 10-cm culture dishes or 2-well chamber slides to a density of $1x10^6$ cells per well or $1x10^5$ cells per well, respectively, and cultured in complete medium for 24 hours. The cells were extensively washed with serum-free medium-199 and then incubated for 24 hours in serum-free medium-199. All floating and adherent cells in a 10 cm culture dish were stained with fluorescein isothiocyanate (FITC)-conjugated annexin V and propidium iodide (PI) using a commercially available kit (Amersham) as previously described [35]. Thereafter, samples were analyzed by flow cytometry (FACScaliber, Becton Dickinson) for viable (annexin V-negative and PI-negative), early apoptotic (annexin V-positive, PI-negative), and late apoptotic/secondary necrotic (annexin V-positive and PI-positive) cells. The extent of the apoptosis (N%) was quantified as a percentage of annexin-V-positive cells [35]. Apoptosis was also assayed by a terminal deoxynucleotidyl transferase mediated biotin nick end-labeling (TUNEL) staining method with a commercial kit (Takara). After removal of the floating cells, the adherent cells in a 2-well chamber slides were fixed and stained according to the supplier's instructions. The mean number of apoptotic (TUNEL-positive) cells from 3 random fields (40 x) in each well was calculated.

***In Vitro* Angiogenesis Model**

Formation of capillary-like structures by HUVECs was assessed on growth factor-reduced Matrigel, a basement membrane matrix preparation (Becton Dickinson). HUVECs were incubated with medium-199 containing 0.5% FCS for 6 hours, after which the HUVECs were plated onto Matrigel (250 µl)-coated 24-well

plates or 4-well chamber slides to a density of $5x10^4$ cells per well and incubated in medium-199 containing 0.5% FCS for 1 hour. Unattached cells were then removed by gentle aspiration, and the medium was replaced with medium-199 containing recombinant human IgG_1 Fc (IgG Fc) (R&D) or recombinant human Tie2/Fc chimeric protein (Tie2/Fc) (R&D). In another set of experiments, HUVECs were incubated with the CM from SeV/Id1-HUVECs (SeV/Id1-CM) or SeV/Null-HUVECs (SeV/Null-CM) in the presence or absence of IgG_1 Fc or Tie2/Fc. Formation of tube/cord-like structures was evaluated 8 hours later. The cultures were photographed with a CCD camera (Olympus), and using NIH Image software the total length of the tube/cord-like structures was quantified as an indicator of angiogenesis. The mean value from 5 random fields (40 x) in each well was calculated.

In Vivo Angiogenesis Model

Animal care and use in our laboratory were in strict accordance with the guidelines for animal and recombinant DNA experiments put forth by Kumamoto University. Male athymic mice (BALB/c, 8-10 weeks old) or male C57BL/6J mice (16-20 weeks old) were anesthetized with intraperitoneal injection of 160 mg/kg pentobarbital. Hindlimb ischemia models were created as follows: for the athymic mouse hindlimb ischemia model the femoral artery and vein were excised, from just above the deep femoral arteries to the popliteal artery and vein, and for the C57BL/6J mouse hindlimb ischemia model [36], all the vessels from the right external iliac artery and vein to just above of the bifurcation of the saphenous and popliteal arteries and veins, including all side branches were ligated, cut, and excised. For cell transplantation intervention, $1x10^5$ HUVECs were suspended in 50 μL of serum-free medium-199 and the solution was injected into 5 different areas of the leg muscles (3

in the thigh and 2 in the calf, 10 μL each) 1 day after the surgical procedures. Blood flow recovery following ischemia was serially evaluated with laser Doppler perfusion imaging (LDPI) (Moor Instruments) over the course of 3 weeks, postoperatively, as previously described [36]. To minimize signal variation caused by variations in ambient light and temperature, calculated blood perfusion (relative units) was expressed as the ischemic (right)/normal (left) limb blood perfusion ratio. At the end of the study, tissue samples were harvested from the lower calf and thigh muscles for histological analysis.

For transplanted HUVEC tracking, HUVECs were labeled with a red fluorescent marker, PKH26-RED (Sigma) according to the supplier's instructions. The labeled HUVECs were rinsed, resuspended in serum-free medium-199, and then transplanted into the hindlimb muscles of a subgroup of mice as described above. For another cell tracking study, a subgroup of mice received an intracardiac injection of FITC-conjugated *Bandeiraea simplicifolia* lectin I (BS-1; Sigma) and rhodamine-conjugated UEA-1 (Sigma) simultaneously or of FITC-conjugated UEA-1 (Sigma) only at 30 minutes before sacrifice [37].

To evaluate endogenous Id1 expression levels, the limb sections were obtained from ischemic limb muscle of C57BL/6J mice at 0, 3, and 14 days after induction of ischemia.

Histological Analysis

Tissue samples harvested from the hindlimb muscles were snap-frozen with pre-cooled isopentane in liquid nitrogen, after which they were embedded in OCT compound (Miles) and cut into 5 to 7-μm-thick sections. For evaluation of capillary density, serving as an anatomic index of angiogenesis, capillary ECs were detected by

staining tissue sections for alkaline phosphatase (AP) with the iodoxyltetrazolium method [36] and counterstaining with eosin. Some additional sections were stained with anti-mouse CD31 antibody to further confirm the EC phenotype. The capillary ECs were then counted under light microscopy (100 x) to determine capillary density. In each animal, 6 different fields of a section were randomly selected for EC counts, which were then averaged. Tissue sections obtained from hindlimb muscles transplanted with PKH26-RED-labeled HUVECs were also stained for AP to detect viable ECs immediately after being photographed with a CCD camera (Olympus). Tissue sections obtained from hindlimb muscles after pre-mortem lectin staining were observed with a computer-assisted microscope (Nikon) (400 x), and UEA-1-positive HUVECs were counted (200 x) to quantify the incorporation of HUVECs into the murine vasculature. For each animal, 3 different fields of a section were randomly selected for cell counting. Tissue sections from hindlimb muscles treated only with UEA-1 were stained with anti-human vWF to further confirm the incorporation of HUVECs into the endothelial layer.

To evaluate the percentage of the SeV-transfected population in HUVECs incorporated into the ischemic limbs, the limb sections were double-immunostained with anti-human CD31 and anti-SeV antibodies. The numbers of human CD31- and/or SeV-positive cells were counted for the sections randomly obtained from 3 different animals.

To evaluate the proliferative state of the transplanted HUVECs, the limb sections were double-immunostained with an anti-human Ki67 antibody and UEA-1. The numbers of human Ki67- and/or UEA-1-positive cells were counted in the sections randomly obtained from 2 different animals.

To evaluate endogenous Id1 expression, the limb sections were

immunostained with anti-Id1 antibody, subsequently amplified the signal with an avidin-biotin complex system using a Vectastain ABC kit (Vector) and counterstained with eosin. The adjacent section was immunostained with anti-mouse CD31 antibody to evaluate EC phenotype.

Statistical Analysis

Each assay experiment was performed at least 3 times. Data were expressed as means ± SD. Student's *t*-test was used to compare continuous values between 2 groups. Differences in limb outcome between 2 groups were analyzed by the χ^2 test. Values of $P<0.05$ were considered to represent statistically significant differences.

VII. Results

Endogenous Id1 Gene Expression Under Ischemia

To investigate endogenous expression levels of Id1 under ischemia, I first analyzed those with immunohistochemical technique in the tissue sections of limbs of C57BL/6J strain mice 3 and 14 days after induction of ischemia. Adjacent sections were immunostained with anti-mouse CD31 antibody to confirm EC phenotype. Analyzing blood flow of ischemic limbs with LDPI showed that recovery of blood flow, reflecting ischemic status of the limb, was accelerated and reached plateau levels 3 and 14 days after ischemia, respectively, as shown in Figure 5I. I observed Id1 expression in only small subset of cells of the limbs, a part of which is EC positive for CD31, 3 and 14 days after ischemia, but did not observe significant differences in Id1 expression levels between 3 and 14 days after ischemia (Figure 5A to 5H).

I next examined Id1 expression levels in cultured HUVECs treated with DFX, an agent mimicking hypoxic condition. RT-PCR analysis showed that VEGF expression was dose-dependently upregulated in HUVECs 24 hours after treatment of DFX. In contrast, real-time PCR analysis showed that expression levels of Id1 were time-dependently decreased in HUVECs by DFX treatment (Figure 5J). These results suggest that Id1 expression is not significantly induced in ischemic limb.

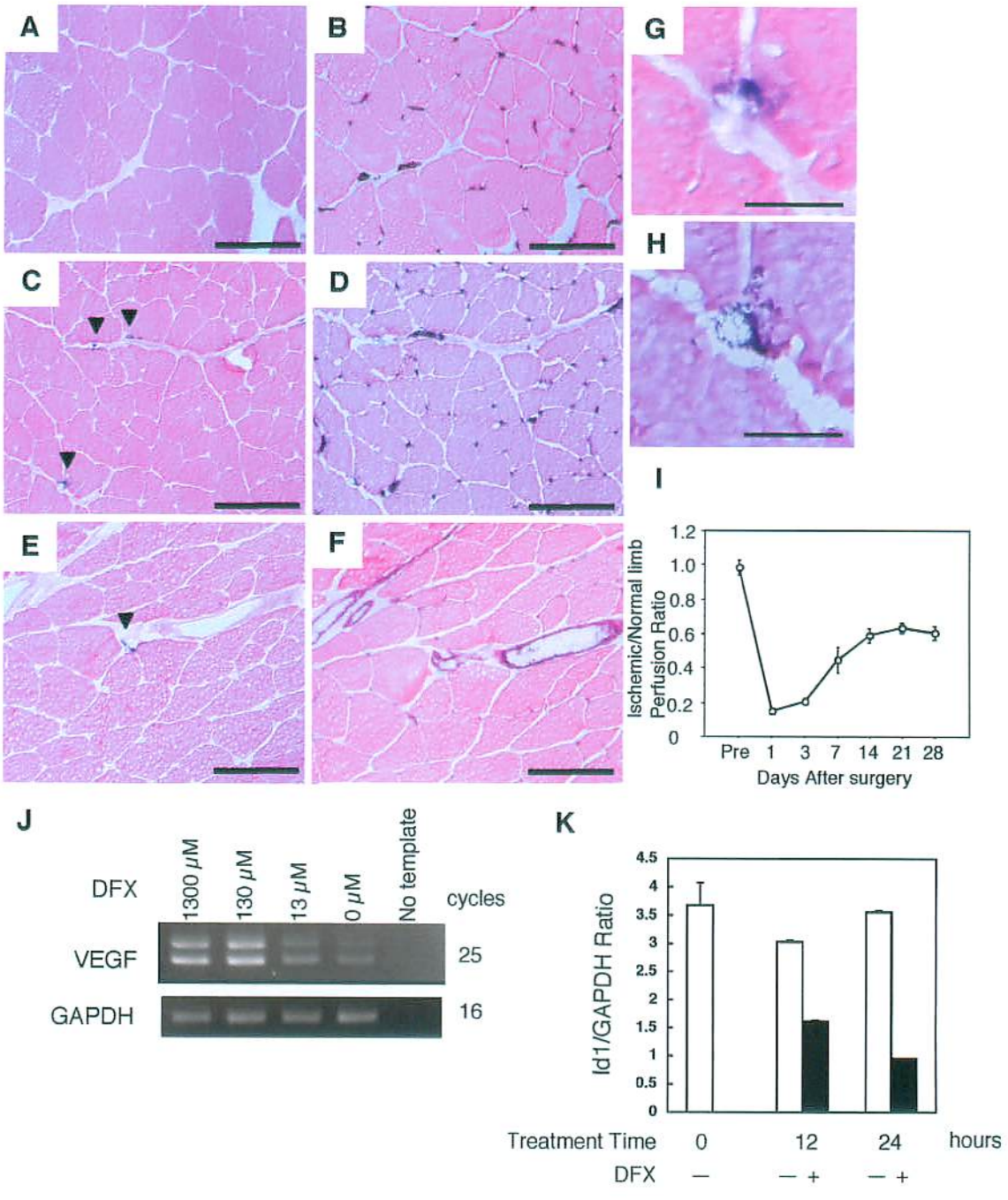

Figure 5. Endogenous Id1 expression under ischemia. A-H, Endognous Id1 levels were examined in the limb section of murine ischemic muscle 0, (A), 3 (C, G), and 14 (E) days after induction of ischemia. The adjacent sections were stained for the detection of CD31 expression, a marker of EC (B, D, F, H, respectively). Id1 expression (arrowheads) was observed in only small subset of cells of the limbs, a part of which is EC positive for CD31, 3 and 14 days after ischemia, but there were no significant differences in Id1 expression between 3 and 14 days after ischemia. Bar=100 μm (A to F) and 20 μm (G, H). I, Ischemia/normal limb perfusion ratios, reflecting blood flow recovery, was evaluated by LDPI. J, K, Analysis of Id1 expression levels in cultured HUVECs treated with DFX. RT-PCR analysis showed that VEGF expression was dose-dependently upregulated in HUVECs 24 hours after DFX treatment (J). In contrast, real-time RT-PCR analysis showed that expression levels of Id1 were time-dependently decreased in HUVECs by DFX treatment (K).

SeV-Mediated Id1 Gene Expression and Protein Synthesis

SeV-mediated Id1 gene expression and protein synthesis in HUVECs were examined by RT-PCR, Western blot and immunocytochemical analyses. Immunostaining for SeV confirmed that ≈ 70% of HUVECs had been successfully infected with SeV within 2 days. RT-PCR confirmed the presence of SeV-mediated Id1 mRNA in HUVECs infected with SeV/Id1 (SeV/Id1-HUVECs) 2 days after transfection, but not in HUVECs transfected with SeV/Null (SeV/Null-HUVECs) (Figure 6A). Western blot analysis with anti-Id1 antibody detected a 14-kDa protein in the cell lysates of SeV/Id1-HUVECs (Figure 6B). In SeV/Id1-HUVECs, Id1 was predominantly localized to the nucleus (Figure 6C).

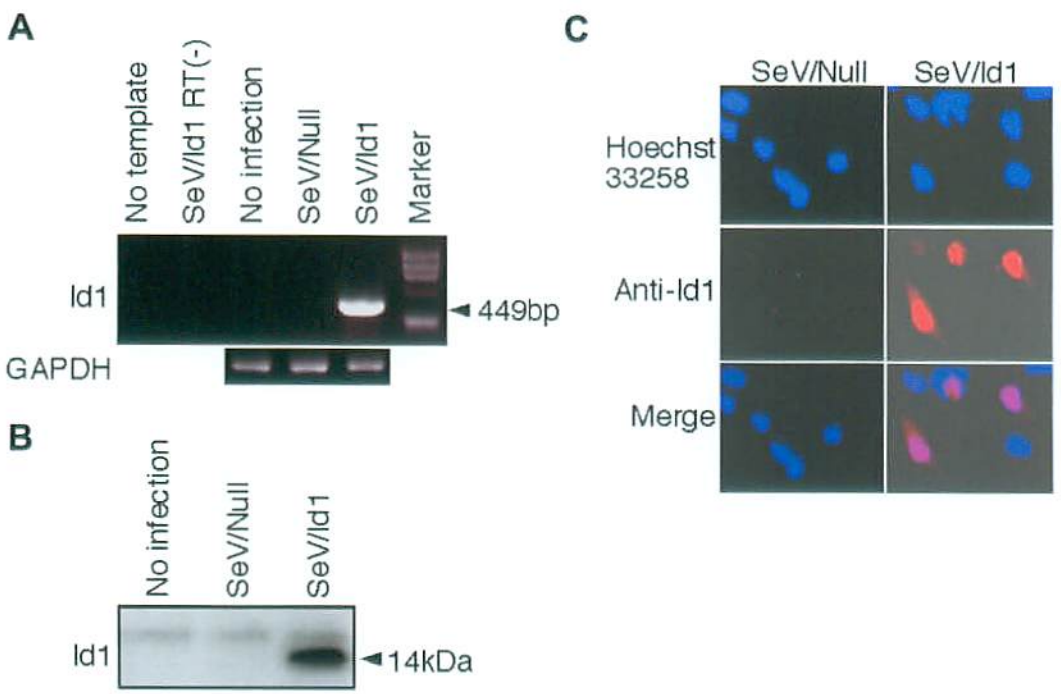

Figure 6. Id1 gene transfer into HUVEC using the SeV vector system. Id1 gene and protein expressions were examined in SeV/Id1-HUVECs 2 days after transfection. A, RT-PCR analysis detected SeV-mediated murine Id1 mRNA in SeV/Id1-HUVECs but not in controls (30 cycles for Id1 and 25 cycles for GAPDH). B, Western blot analysis confirmed Id1 protein synthesis in SeV/Id1-HUVECs. C, Immunocytochemical staining for Id1 showed localization of Id1 primarily in the nucleus in SeV/Id1-HUVECs with less in the cytoplasm.

Effects of Serum Stimulation on Endogenous Id1 Expression in HUVECs

Id1 was endogenously expressed in HUVECs (data not shown) and the expression has been reported quite responsive to serum [38]. Therefore, I examined endogenous Id1 levels of HUVECs in the presence or the absence of FCS by real-time PCR technique. I stimulated HUVECs with 0% FCS, 0.5 % FCS, 5% FCS, or 10% FCS, and obtained total RNA samples before and 1 and 6 hours after the stimulation. Endogenous Id1 levels were abruptly and does-dependently increased with serum stimulation, whereas those were decreased by serum deprivation for 1 hour (Figure 7). Id1 levels were decreased down to the levels equal to or less than basal levels 6 hours after serum stimulation (Figure 7). In the case of the stimulation with 0.5% FCS, Id1 levels were decreased down to the equal levels to those in serum deprivation 6 hours after the stimulation (Figure 7). Therefore, I preformed nearly all following *in vitro* experiments 6 hours after serum deprivation of 0.5% FCS-added medium-199.

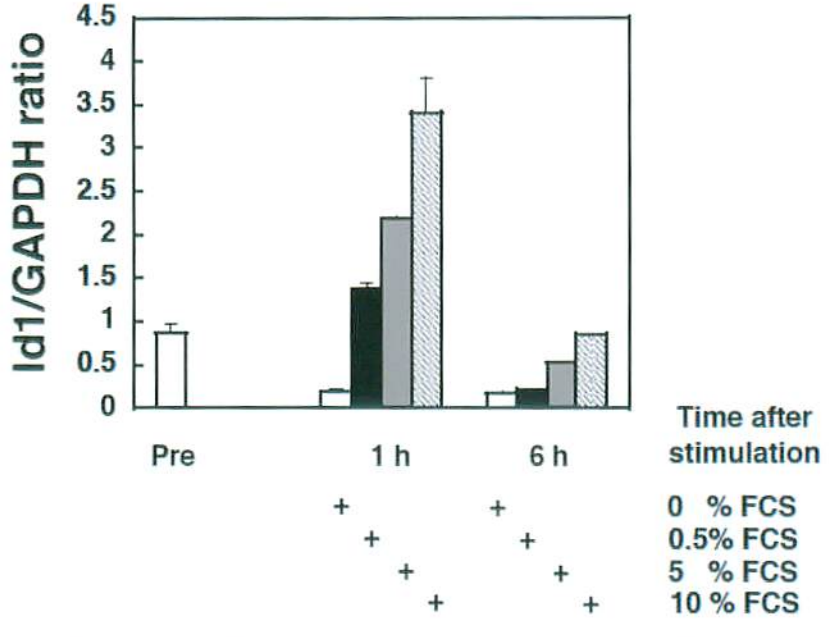

Figure 7. Influences of serum stimulation on endogenous Id1 mRNA levels in HUVECs. Id1 levels were quite responsive to serum stimulation. However, endogenous Id1 levels were not significantly affected by addition of 0.5% FCS and following incubation for 6 hours.

Id1 Gene Transfer Confers Angiogenic Activity on HUVECs

To examine the angiogenic effect of Id1 gene transfer, scratch wound assays were performed on HUVECs under serum-reduced and growth factor-free conditions. Id1 increased HUVEC migration up to 144 % of the control level after 24 hours ($P<0.05$) (Figure 8A, 8B), as previously reported in other types of ECs [25, 39]. Id1 gene transfer also stimulated cell growth irrespective of the presence of VEGF as estimated by BrdU incorporation (Figure 8C).

In the Matrigel tube formation assay, SeV/Id1-HUVECs formed robust elongated tube/cord-like structures (Figure 9A). Quantitative analysis showed total tube/cord lengths to be significantly greater in the SeV/Id1-HUVECs than in the SeV/Null-HUVECs ($P<0.01$) (Figure 9B). Furthermore, I detected cavity-like structure in the coronal section of tube-like structure of HUVECs on Matrigel by HE staining (Figure 9C). These findings clearly suggest that Id1 gene transfer confers angiogenic activity on HUVECs *in vitro*.

Id1 Gene Transfer Protects Against HUVEC Apoptosis

Previous reports have suggested that Id1 can both positively and negatively regulate apoptosis depending on cell types [40, 41]. To examine the effects of Id1 on EC apoptosis, I cultured HUVECs in serum-free medium in the presence or absence of SeV/Id1 and evaluated apoptotic cells using flow cytometry. Id1 gene transfer reduced the number of annexin V-positive cells to 47% of the control level (Figure 10A). TUNEL staining also showed that Id1 significantly reduced the number of TUNEL-positive cells down to 40% of the control number (Figure 10B). Representative images of HUVECs with TUNEL staining are shown in Figure 10C. These results show clearly that Id1 can protect HUVECs against apoptosis *in vitro*.

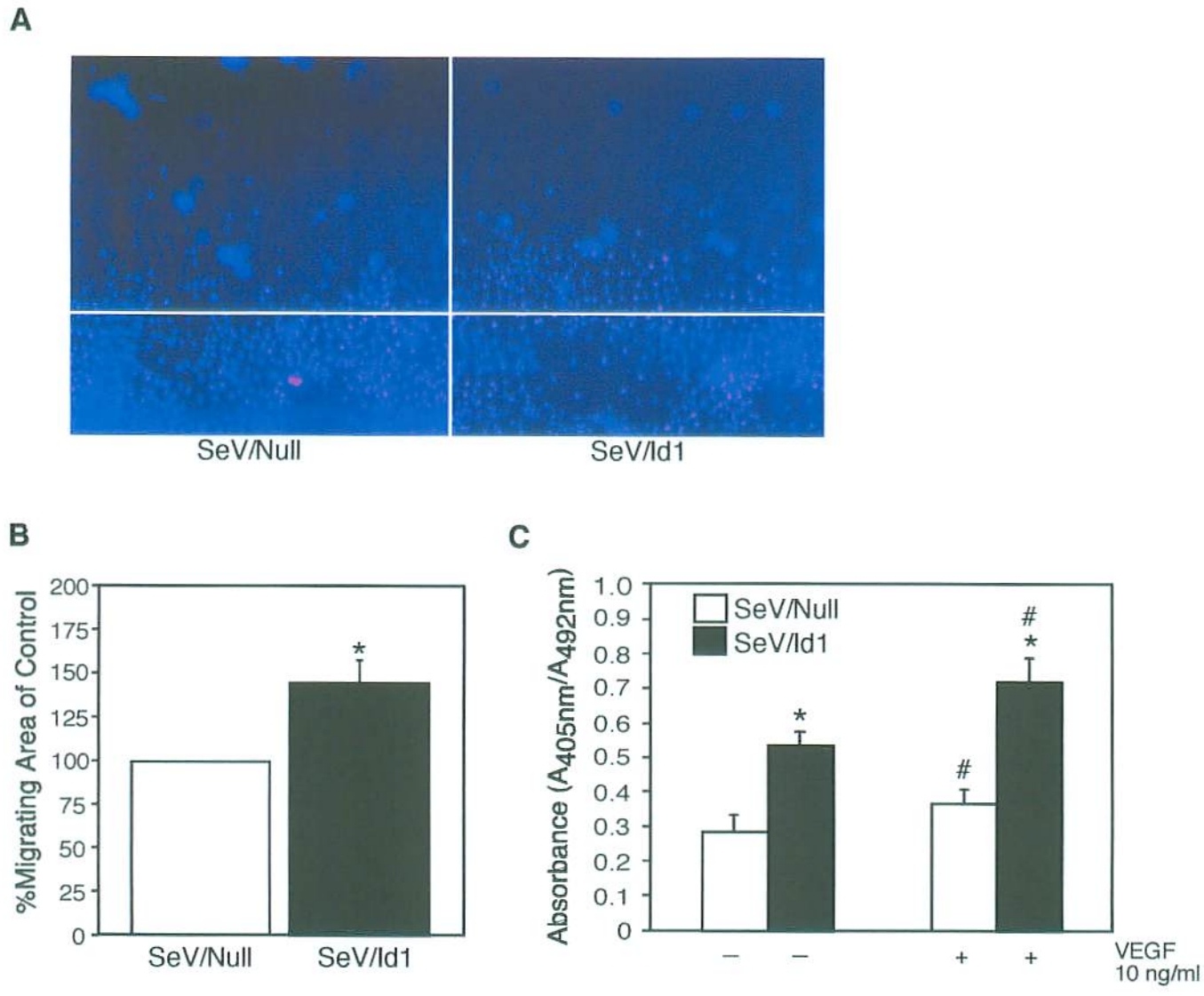

Figure 8. Increased migratory and proliferation properties of SeV/Id1-HUVECs. A, B, Scratch wound assay. Representative photographs of nuclear staining (DAPI) of migrated HUVECs 24 hours after scraping a portion of the cell monolayer away (A). White lines indicate the edge of the injured monolayer (starting point). Scratch wound assay showed that Id1 had increased HUVEC migration up to 144 % of the control level by 24 hours (n=4 each). *P<0.05 vs. SeV/Null. C, BrdU incorporation assays showed that DNA synthesis was increased in SeV/Id1-HUVECs (n=5) irrespective of the presence of VEGF. * P<0.01 vs. SeV/Null. #P<0.01 vs. no VEGF treatment.

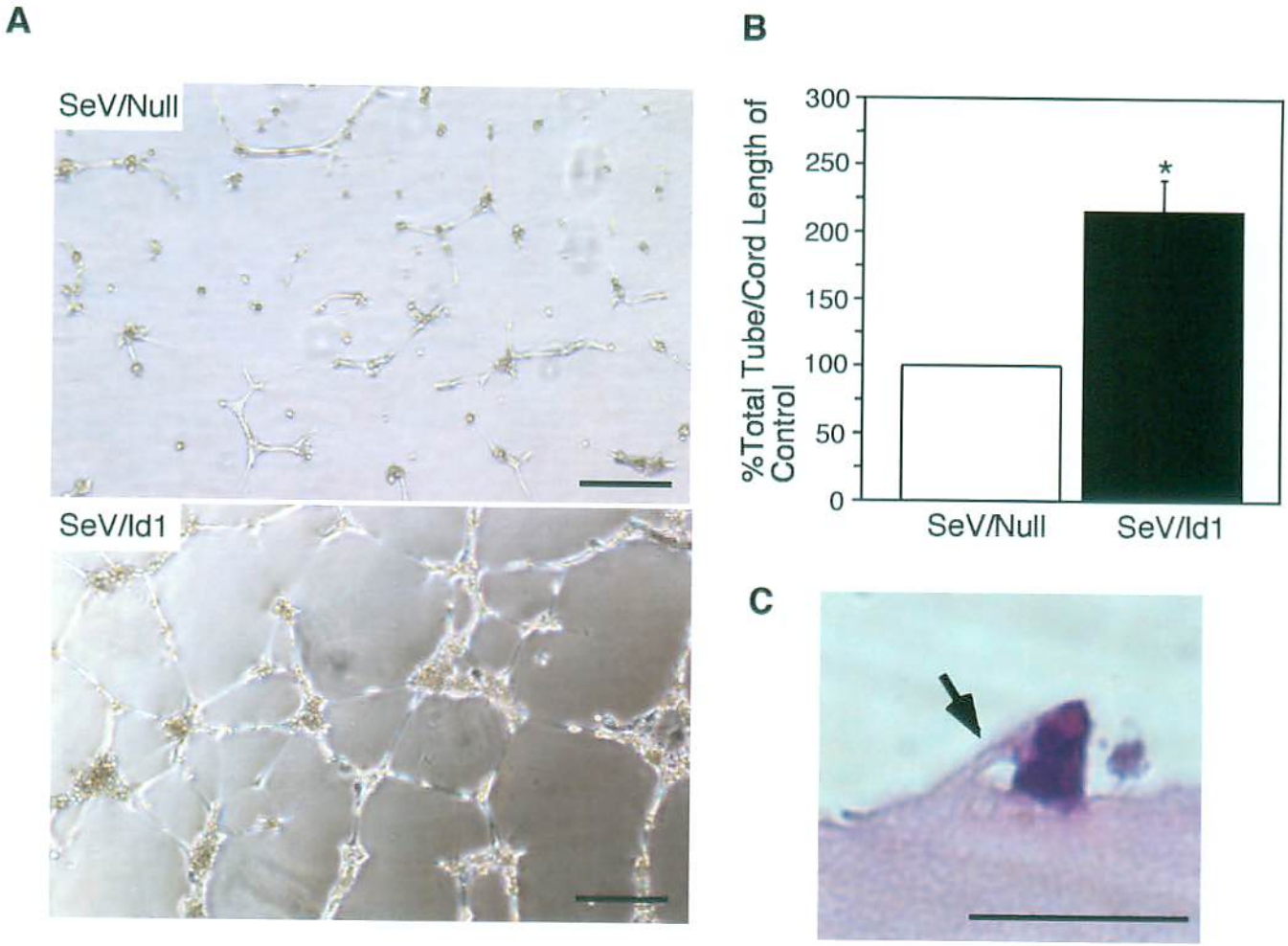

Figrure 9. Enhanced angiogenic phenotype of SeV/Id1-HUVECs. A, Representative photographs of capillary-like tube/cord formation of SeV/Null- and SeV/Id1-HUVECs on Matrigel. In comparison to SeV/Null-HUVECs, SeV/Id1-HUVECs formed robust elongated tube/cord-like structures. Bar=100 μm. B, Quantification of the total tube/cord length of capillary-like structures. The total tube/cord lengths were significantly greater in SeV/Id1-HUVECs (n=4) than in SeV/Null-HUVECs (n=4). * $P<0.01$ versus SeV/Null. C, A representative photograph of the coronal section of tube-like structure of HUVECs on Matrigel with HE staining. Cavity-like structure (arrow) was detected in the coronal section. Bar=25 μm.

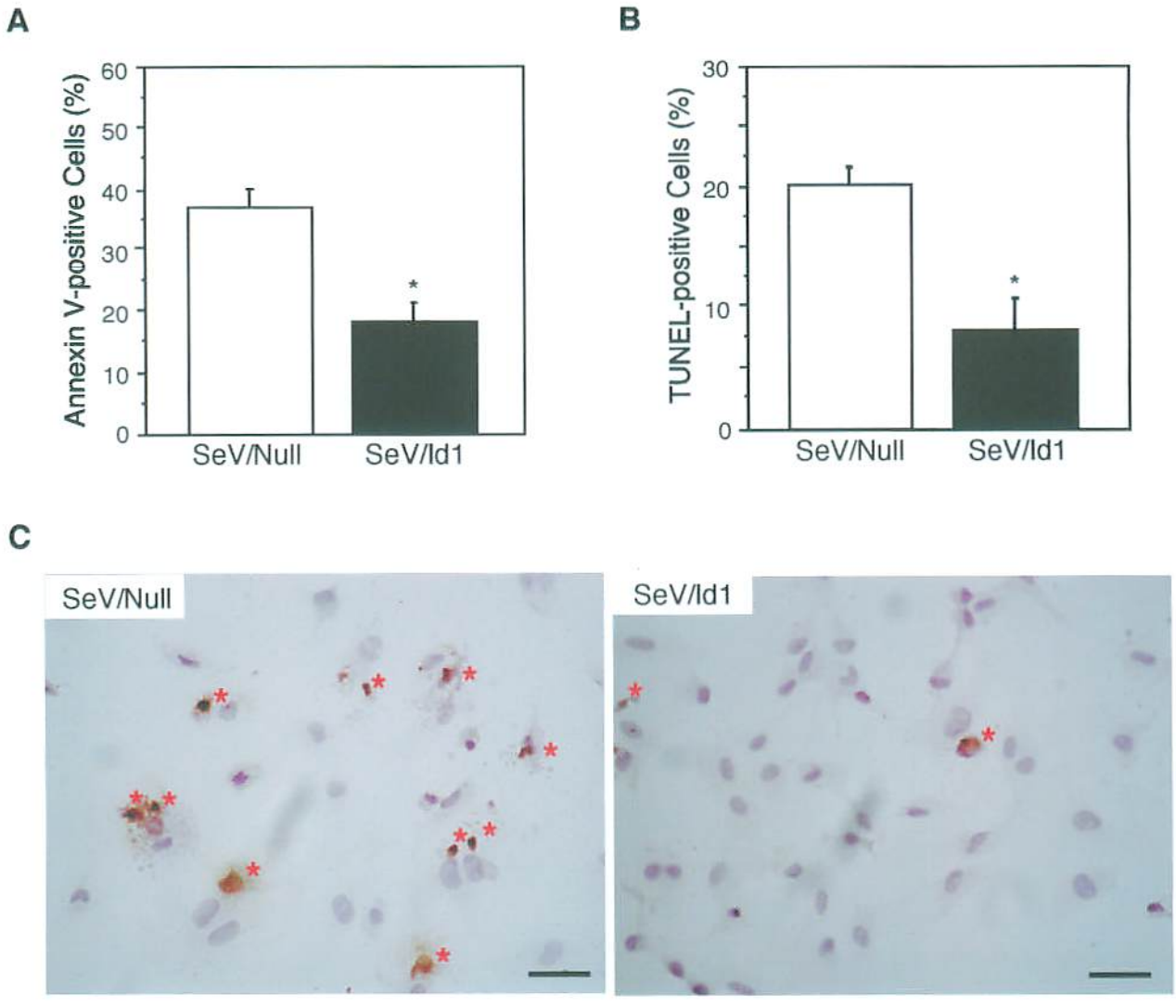

Figure 10. Inhibitory effects of Id1 gene transfer on apoptosis in HUVECs. Cellular viability was estimated after 24 hours of serum deprivation. A, Flow cytometric analysis with anti-annexin V antibody showed a smaller population of annexin V-positive cells (apoptotic cells) among the SeV/Id1-HUVECs (n=5) than among the SeV/Null-HUVECs (n=5). *P<0.01 vs. SeV/Null. B, TUNEL staining of cultured HUVECs showed a smaller population of TUNEL-positive cells (apoptotic cells) among the SeV/Id1-HUVECs (n=5) than among the SeV/Null-HUVECs (n=5). *P<0.01 vs. SeV/Null. C, Representative images of TUNEL and methyl green staining for the SeV/Null- and SeV/Id1-HUVECs. Red asterisks indicate TUNEL-positive cells. Bar=50 μm.

Establishment of Hindlimb Ischemia Model in Athymic Mice

For the establishment of hindlimb ischemia model in athymic mice of BALB/c strain, I first generated ischemia in similar manner with C57BL/6 mice [36]. By this method, among C57BL/6 mice femoral artery resection rarely led to limb necrosis, not even of the toes; whereas among BALB/c athymic mice it led to extensive necrosis of the limb in more than 50% of mice within 3 days. To permit limb survival at least beyond 3 days and to evaluate the effects of cell transplantation on ischemic limbs, I therefore modified the conventional method to resect the femoral artery as described in the Materials and Methods section.

Transplantation of Id1-Transfected HUVECs Augments Revascularization of Murine Ischemic Hindlimbs

I assessed the angiogenic potency of Id1-transfected HUVECs for therapeutic purposes by transplanting them into murine ischemic hindlimbs. One day after surgical induction of ischemia, $1x10^5$ HUVECs were directly transplanted into the hindlimb muscles of the athymic mice. Blood perfusion recovery after transplantation was then serially assessed with LDPI. Ischemia/normal limb perfusion ratios before surgery were similar in the treatment groups: medium (n=14), SeV/Null-HUVECs (n=11), and SeV/Id1-HUVECs (n=14) (Figure 11A). Immediately after surgery, limb perfusion was severely reduced in all groups to the same extent (Figure 11A), indicating the ischemia severities to be comparable. Over the next 21 days, LDPI revealed gradual recovery of blood perfusion in all 3 groups. Remarkably, recovery was accelerated in the SeV/Id1-HUVECs group. Ischemia/normal limb perfusion ratios on postoperative days 14 and 21 (0.71 ± 0.25 and 0.71 ± 0.12, respectively) were significantly higher in transplanted hindlimbs than in those of the medium-only

(0.46±0.18, $P<0.01$ and 0.48±0.20, $P<0.01$, respectively) and SeV/Null-HUVECs (0.52±0.20, $P<0.05$ and 0.54±0.13, $P<0.01$, respectively) groups (Figure 11A). Recovery of blood perfusion was similar in the SeV/Null-HUVECs and medium-only groups. I also examined increases in transplanted cell numbers up to $5x10^5$ cells and obtained similar results (data not shown). Representative images of hindlimb blood perfusion recorded 21 days after surgical induction of ischemia are shown in Figure 11B.

I then examined whether the recovery of blood flow in this ischemic hindlimb model had resulted from neovascularization. Figure 11C represents photomicrographs of representative ischemic limb sections obtained on day 21. Consistent with the LDPI analysis, immunohistochemical staining for AP revealed larger numbers of capillary ECs in the hindlimbs of the SeV/Id1-HUVECs group (80.5±12.8 number per field) than in the medium-only (47.2±10.5, $P<0.01$) and in the SeV/Null-HUVECs (43.2±10.5, $P<0.05$) groups, but there was no significant difference between the latter 2 (Figure 11D).

Increased neovascularization in the mouse ischemic hindlimb can potentially lead to important biological consequences, including limb salvage. To examine limb outcome after induction of ischemia, the appearance of the ischemic hindlimb was observed on the last day of the study period (day 21 after surgery). Among 14 mice in the medium-only group, 7 (50.0%) showed toe necrosis and 1 (7.1%) showed severe limb necrosis, including auto-amputation (Figure 11E). Only 6 (42.9%) were devoid of necrotic lesions (Figure 11E). In contrast, transplantation of SeV/Id1-HUVECs significantly increased the rate of complete limb salvage up to 92% (Figure 11E). Transplantation of SeV/Null-HUVECs did not improve limb outcomes (Figure 11E). Taken together, these findings indicate that transplantation of SeV/Id1-

HUVECs, but not of SeV/Null-HUVECs, can rescue ischemic lesions, and thereby prevent catastrophic outcomes, by augmenting neovascularization.

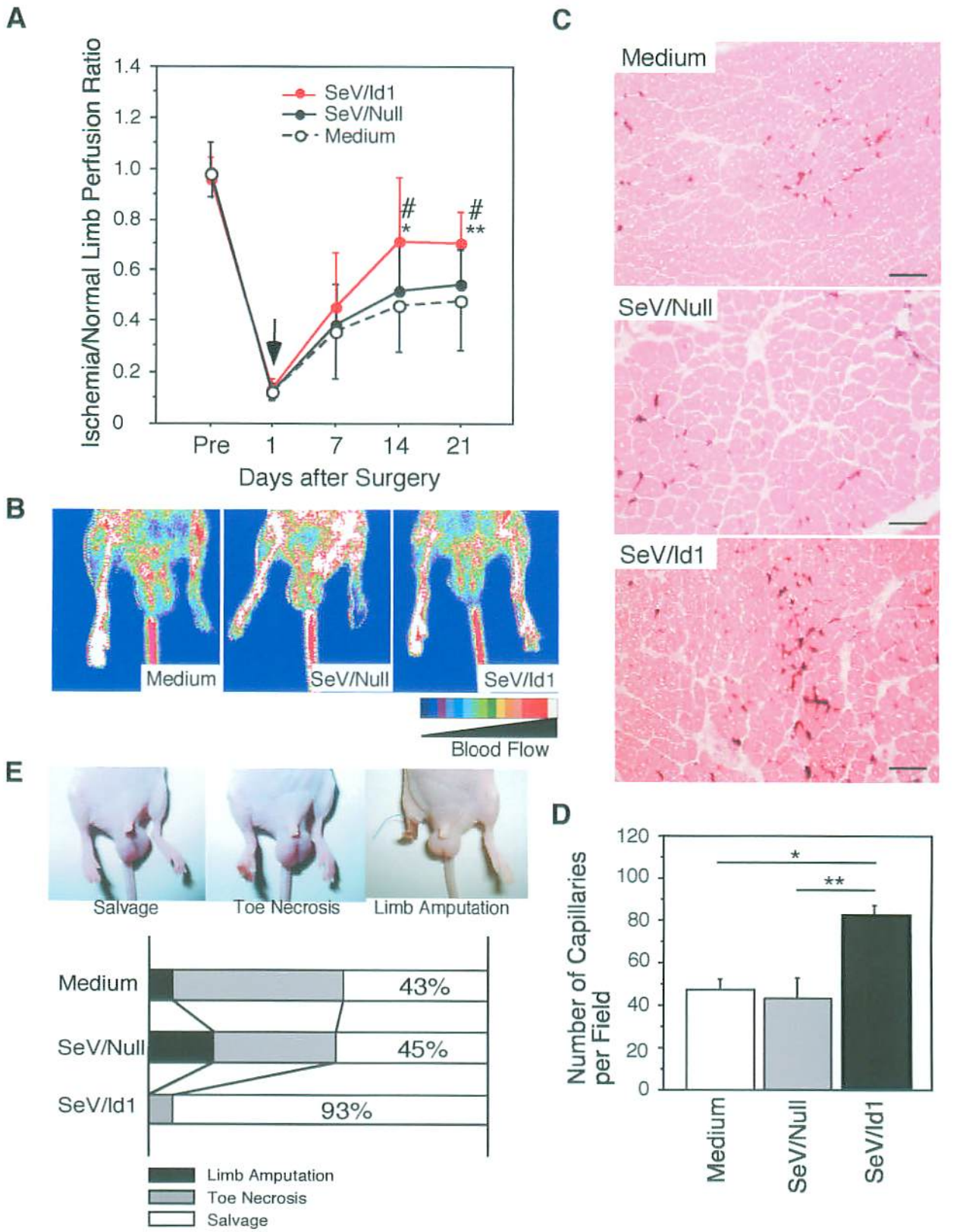

Figure 11. Effects of transplantation of SeV/Id1-HUVECs in murine hindlimb ischemia model. A, Ischemia/normal limb perfusion ratios, reflecting blood flow recovery, on postoperative days 14 and 21 were significantly higher in the SeV/Id1-HUVECs group (n=14) than in the medium-only (n=14) and SeV/Null-HUVECs (n=11) groups, but the difference between the latter 2 groups was not significant. Arrow indicates the day of treatment. *P<0.05, **P<0.01 vs. SeV/Null and #P<0.01 vs. Medium. B, Representative LDPI images recorded 21 days after surgical induction of ischemia. In the digital color-coded images shown, red, yellow and blue indicate regions with maximal, intermediate and minimal perfusion, respectively. C, Representative images of AP staining of sections harvested from an ischemic hindlimb 21 days after surgical induction of ischemia. Bar=100 μm. D, Capillary densities of the sections were greater in the SeV/Id1-HUVECs group (n=4) than in the medium-only (n=4) and SeV/Null-HUVECs (n=4) groups, but there was no significant difference between the latter 2. *P<0.05, **P<0.01. E, Limb outcomes 21 days after surgical induction of ischemia. Representative photographs of limb outcomes: salvage, toe necrosis and auto amputation (upper panel). The complete limb salvage rate was higher in the SeV/Id1-HUVECs group (n=14) than in the SeV/Null (n=11, P<0.01) and medium-only (n=14, P<0.01) groups (lower panel).

Evidence of Incorporation of Transplanted HUVECs Into Murine Hindlimb Vasculature

To determine whether transplanted HUVECs contribute to vascular structure regeneration, I labeled HUVECs with PKH26-RED before transplantation and examined their incorporation into capillaries on day 21. After inspection of tissue sections harvested from the ischemic limb for fluorescent labeled HUVECs, the same sections were stained for AP to detect viable HUVECs. HUVECs double positive for PKH26-RED and AP were documented in the sites of hindlimb capillaries in SeV/Id1-HUVECs, showing incorporation of transplanted HUVECs into the murine hindlimb vasculature (Figure 12A, 12B). To further confirm and quantify these observations, HUVECs and murine ECs were identified using premortem staining by intracardiac injection of fluorescent conjugated lectins (UEA-1 specific for human ECs and BS-1 specific for murine ECs). Stereomicroscopic examination of lectin-stained muscle blocks revealed numerous incorporated HUVECs in the hindlimb vasculature of the SeV/Id1-HUVECs group (Figure 12C to 12E). By contrast, only a few HUVECs were detected in the hindlimb vasculature in the SeV/Null-HUVECs group (Figure 12F). In addition, tissue sections were quantitatively analyzed for incorporated HUVECs. Representative photomicrographs of sections from both groups are presented in Figure 12G, 12H. The number of incorporated HUVECs in the SeV/Id1-HUVECs group was $\approx$ 5 times that of the SeV/Null-HUVECs group (Figure 12I). At higher magnification, the capillary wall proved to be partly composed of UEA-1 positive HUVECs (Figure 12J, 12K). In addition, UEA-1-positive HUVECs resided in the endothelial layer positive for vWF (Figure 12L, 12M). These results confirm that Id1-transfected HUVECs can be effectively incorporated into regenerating capillaries in ischemic lesions.

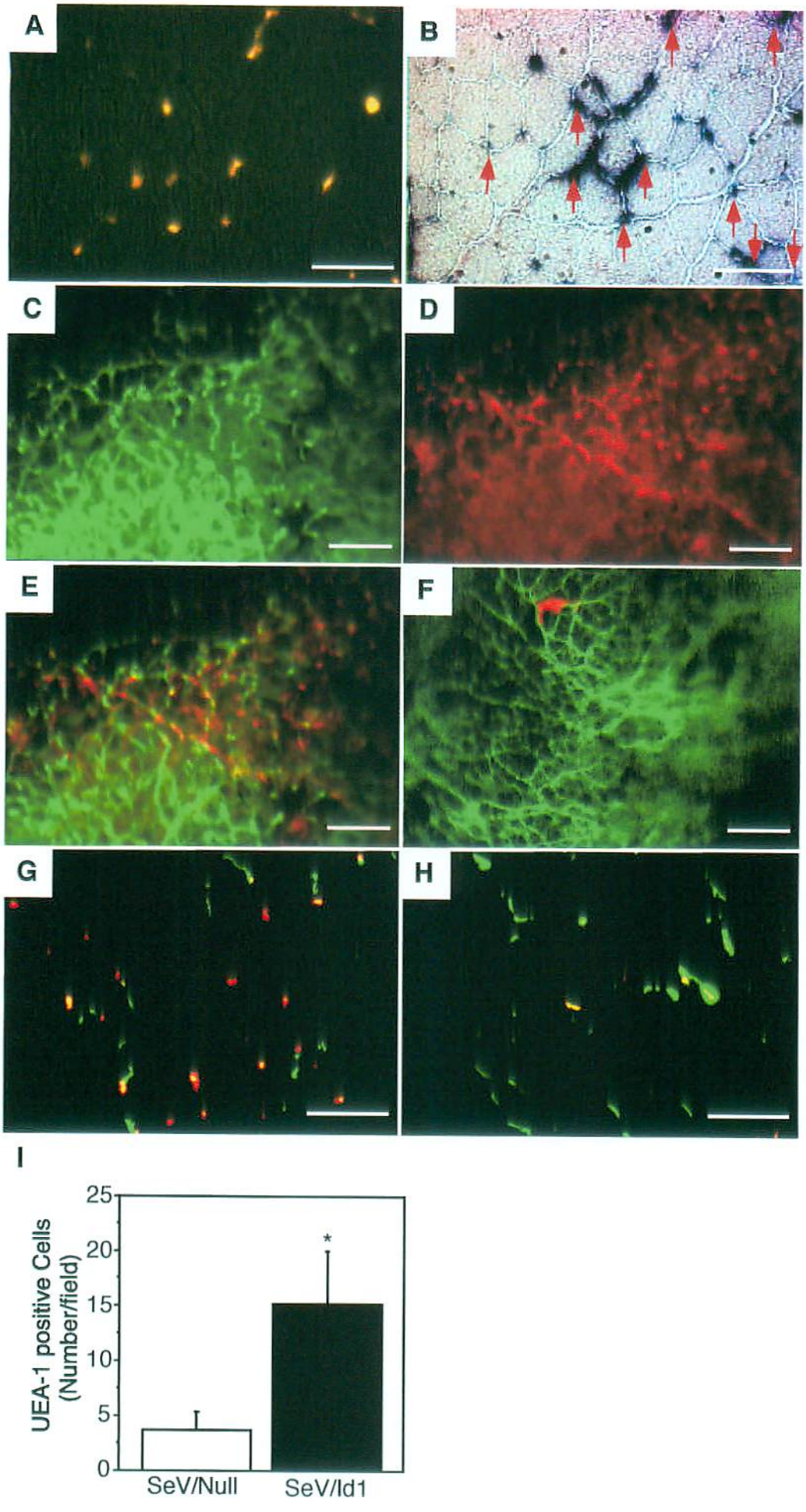
A
B
C
D
E
F
G
H
I
UEA-1 positive Cells
(Number/field)
25
20
15
10
5
0
*
SeV/Null
SeV/Id1

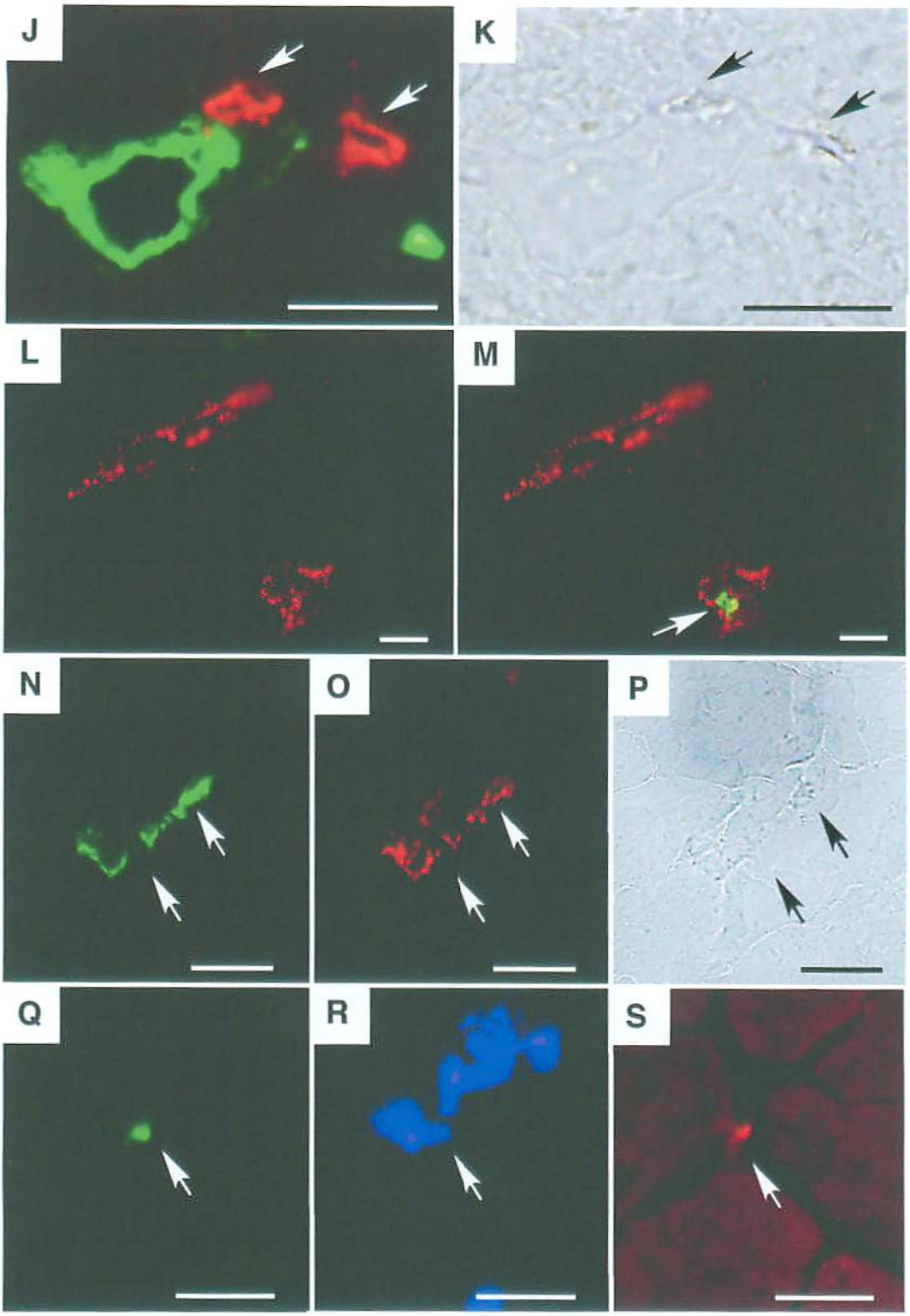

Figure 12. Incorporation of transplanted HUVECs into the vascular network in murine ischemic hindlimbs. A, B, Incorporation of PKH-26-RED-prelabeled SeV/Id1-HUVECs. The same section of murine ischemic muscle 21 days after transplantation was examined for the PKH-26-RED signal (A) and stained for AP activity (B). Arrows indicate PKH-26-RED-prelabeled HUVECs scattered in the capillary network, as characterized by AP staining. C to F, Stereomicroscopic images of lectin-stained vascular networks in murine ischemic hindlimbs 21 days after transplantation of SeV/Id1-HUVECs (C to E) and SeV/Null-HUVECs (F). C, BS-1 lectin staining (green); D, UEA-1 lectin staining (red); E, F, merged. G to K, Representative images of tissue sections with pre-mortem BS-1 (green) and UEA-1 (red) lectin staining after transplantation with SeV/Id1-HUVECs (G, J) or SeV/Null-HUVECs (H). I, Quantitative analysis of UEA-1-positive incorporated HUVECs after transplantation. n=4, *P<0.05 vs. SeV/Null. K, Phase contrast image corresponding to J. L, M, Representative images tissue sections with pre-mortem UEA-1 (green, arrow) and post-mortem vWF (red) staining after transplantation with SeV/Id1-HUVECs. L, vWF staining; M, merged. N-P, Representative images of human CD31- (N, green) and SeV- (O, red) positive HUVECs (P, arrows) in the ischemic hindlimb section 14 days after transplantation. Q to S, Representative images of human Ki67- (Q, green) and UEA-1- (S, red) positive HUVECs (arrow) in the ischemic hindlimb section 7 days after transplantation. R, DAPI staining. Bar=100 μm (A to H) and 20 μm (J to S).

To evaluate whether Id1-transfected HUVEC were incorporated into the ischemic limbs, the sections obtained from 14 days after HUVECs transplantation were double-immunostained with anti-human CD31 and anti-SeV antibodies. Cells positive for both human CD31 and SeV were regarded as SeV/Id1-transfected HUVECs. Among 243 HUVECs positive for human CD31, 211 cells (87%) were positive for SeV, indicating that the majority of the incorporated HUVECs overexpressed Id1. Representative photographs of human CD31- and SeV-positive cells are shown in Figure 12N to 12P.

To address the mechanism underlying the *in vivo* effects of Id1, I evaluated whether transplanted HUVECs are in a proliferative state by double-immunostaining the section obtained from hindlimb muscles 7 days after HUVEC transplantation with an anti-human Ki67-antibody and UEA-1. I observed that 6.5 % of UEA-1-positive HUVECs were Ki67-positive in the section from the SeV/Id1-HUVEC group, whereas I did not detect any Ki67-positive HUVECs in the section from the SeV/Null-HUVEC group. A representative photograph of Ki67- and UEA-1-positive cells is shown in Figure 12Q to 12S.

Ang1 Is Upregulated and Functionally Contributes to *In Vitro* Angiogenesis on Id1-Transfected HUVECs

To address the mechanism of the angiogenic potencies in SeV/Id1-HUVECs, the gene expressions of several angiogenic factors and their receptors were assessed on HUVECs 2 days after Id1 gene transfer. Semi-quantitative RT-PCR analysis showed the Ang1 gene, but not the VEGF, Ang2, KDR, Flt-1, or TIE2 gene, to be upregulated on SeV/Id1-HUVECs (Figure 13A). Western blot analysis revealed increased levels of Ang1 protein in the cell lysates of SeV/Id1-HUVECs (Figure 13B).

In addition, co-immunostaining with anti-Ang1 and anti-CD31 antibodies detected Ang1 in the cytoplasm of SeV/Id1-HUVECs (Figure 13C). Staining for SeV/Ang1-transfected HUVECs served as a positive control (Figure 13D).

To evaluate whether upregulated Ang1 functionally contributes to the angiogenic property of SeV/Id1-HUVECs, I examined the effect of Tie2/Fc in a Matrigel tube formation assay. In Matrigel, the formation of elongated tube/cord-like structures in SeV/Id1-HUVECs was suppressed by Tie2/Fc (Figure 14A to 14D). Quantitative analysis showed total tube/cord lengths to be significantly smaller in SeV/Id1-HUVECs treated with Tie2/Fc than in those treated with IgG Fc ($P<0.05$) (Figure 14E). Total tube/cord length remained significantly greater in SeV/Id1-HUVECs treated with Tie2/Fc than in SeV/Null-HUVECs even if the used dosage of Tie2/Fc was increased ($P<0.05$) (Figure 14E). I next evaluated whether SeV/Id1-CM also stimulate tube/cord formation of HUVECs in Matrigel. Total tube/cord lengths of HUVECs on Matrigel were significantly greater in the HUVECs treated with SeV/Id1-CM than in those with SeV/Null-CM ($P<0.01$) (Figure 14F); furthermore, the effects of SeV/Id1-CM on tube/cord formation of HUVECs were again partially suppressed by the presence of Tie2/Fc. A previous study reported that not only Ang1 but also Ang2 might activate Tie2 receptor [42]. Because Ang1 but not Ang2 was upregulated in SeV/Id1-HUVECs in the present study, the inhibitory effects of tube/cord formation by Tie2/Fc were considered due to the suppression of Ang1/Tie2 signaling. Collectively, these results suggest that upregulated Ang1 functionally contributes to the angiogenic effects of Id1 and that additional angiogenic factor(s) may also be upregulated in SeV/Id1-HUVECs.

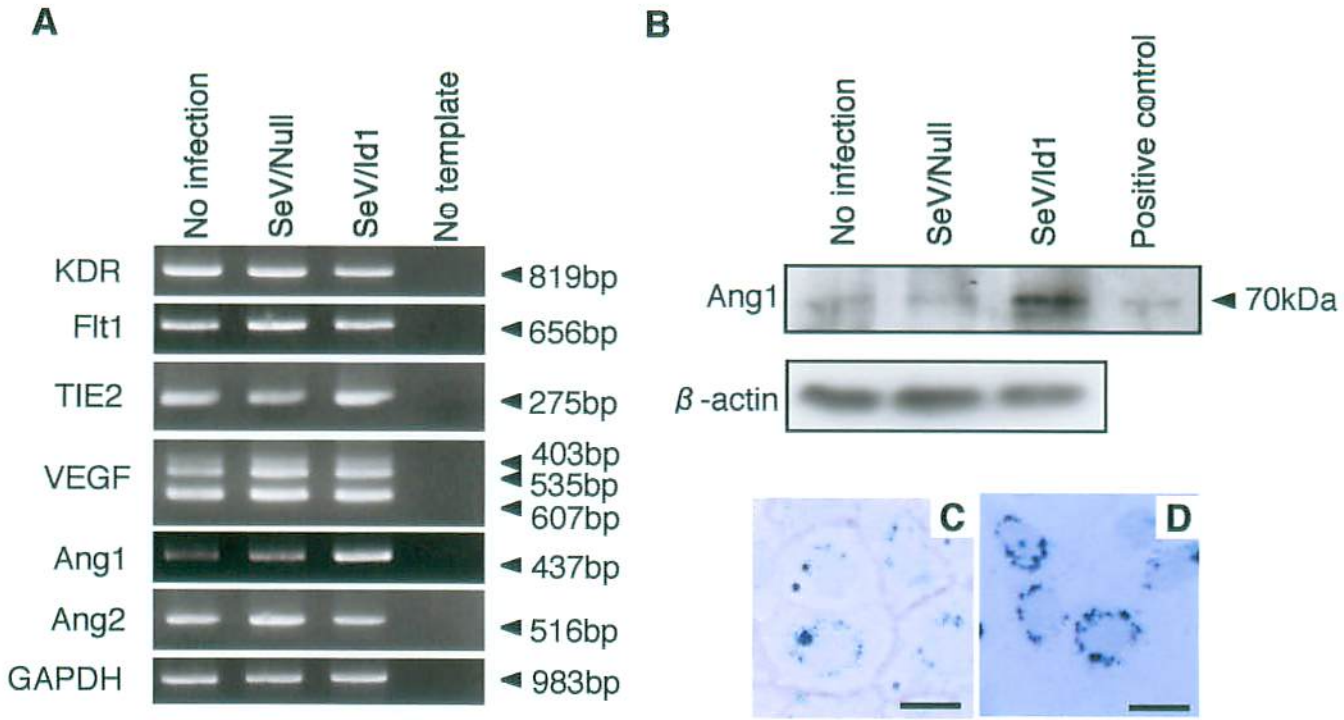

Figure 13. Upregulation of Ang1 expression in SeV/Id1-HUVECs. A, Semi-quantitative RT-PCR demonstrates increased Ang1 expression in SeV/Id1-HUVECs, whereas the expression of VEGF, Ang2, and their receptors was not changed. B, Western blot analysis demonstrates increased Ang1 protein levels in the cell lysates of the SeV/Id1-HUVECs. Conditioned media harvested from COS7 cells infected with SeV/Ang1 was used for positive control. ß-Actin levels served as internal control. C, D, Immunocytochemical staining for Ang1. Double-immunocytochemical staining for Ang1 (blue) and CD31 (brown) confirms Ang1 expression on endothelial cells (C). SeV/Ang1-HUVECs served as positive control for Ang1 staining (D). Bar=40 μm.

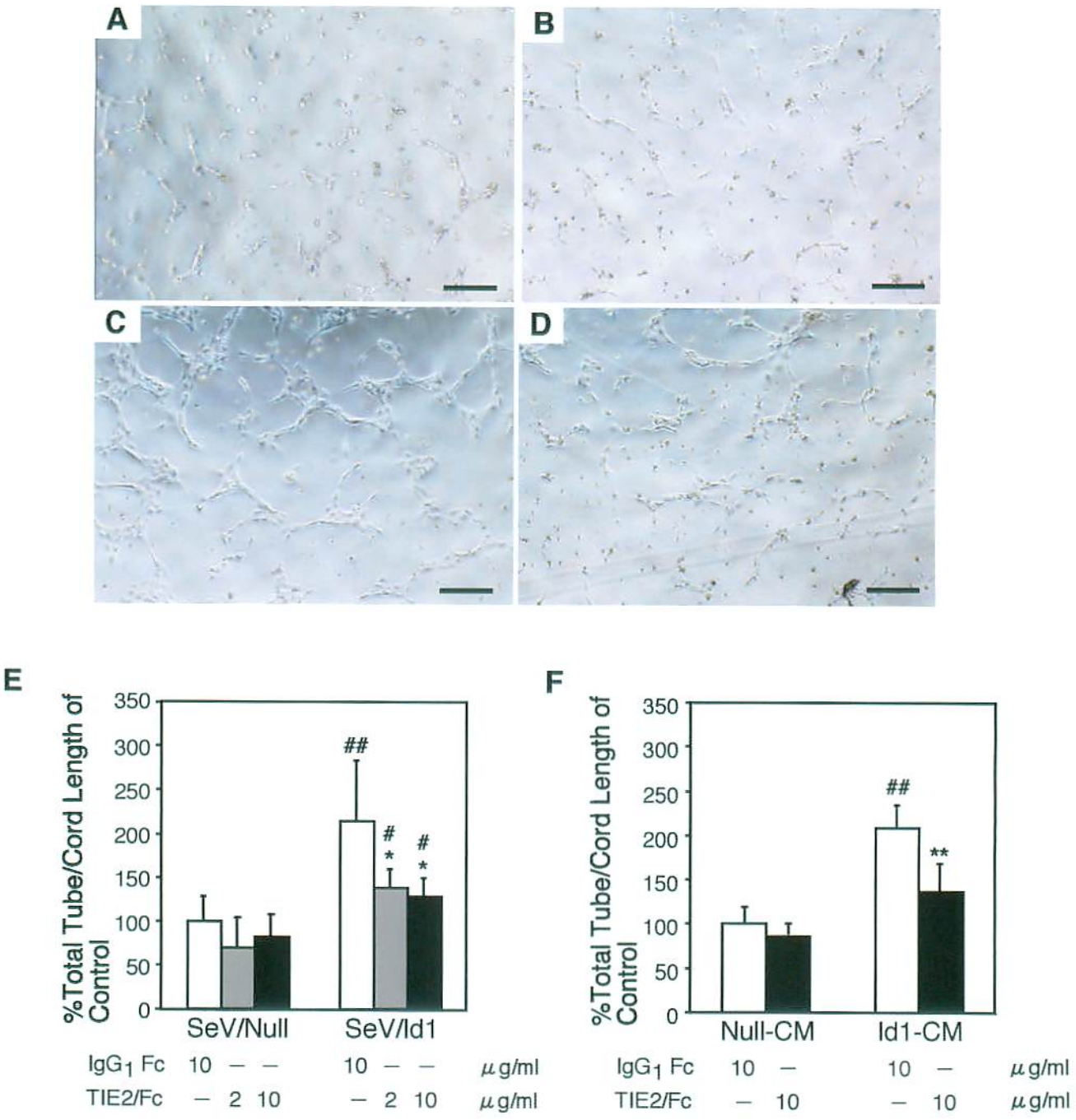

Figure 14. Upregulated Ang1 contributes to enhanced angiogenic property in Id1-transfected HUVECs. A to D, Representative photographs of capillary-like tube/cord formation of SeV/Null- (A, B) and SeV/Id1-HUVECs (C, D) on Matrigel in the presence of 10 μ g/ml IgG_1 Fc (A, C) or 10 μ g/ml Tie2/Fc (B, D). Bar=100 μm. E, Quantification of the total tube/cord length of capillary-like structures. N=8, for each group. * P<0.05 vs. SeV/Id1 treated with IgG_1 Fc. #P<0.05, ##P<0.01 vs. SeV/Null treated with IgG_1 Fc. F. Quantification of the total length of tube/cord like structure in HUVECs treated with SeV/Null- and SeV/Id1-CM in the presence or absence of Tie2/Fc. n=5, for each group. ** P<0.01 vs. SeV/Id1 treated with IgG_1 Fc, ##P<0.01 vs. SeV/Null treated with IgG_1 Fc.

VIII. Discussion

In the present study, I have demonstrated that gene transfer of Id1, a member of the HLH protein family, confers an angiogenic property on HUVECs *in vitro* and *in vivo*. Id1 gene transfer enhanced migration, proliferation and capillary-like tube/cord formation of HUVECs. Id1 gene transfer also protected HUVECs from serum deprivation-induced apoptosis. Transplantation of SeV/Id1-HUVECs accelerated vascular regeneration in the murine ischemic limb and consequently led to limb salvage. Consistently, transplanted SeV/Id1-HUVECs were effectively incorporated into the regenerating vasculature. Finally, I documented upregulation of Ang1 in SeV/Id1-HUVECs, which functionally contributed to enhanced *in vitro* angiogenesis.

In the previous studies [37, 43, 44], the angiogenic potency of EPC was investigated in hindlimb ischemia using a similar mouse model, in which systemic transplantation of *ex vivo* expanded EPCs dramatically accelerated blood flow recovery and increased capillary densities in the ischemic limb. Beneficial effects of local transplantation of EPCs have also been shown in other animal models [45, 46]. Kim and colleagues [16] transplanted ECs isolated form the aorta directly into the scar sites of rat hearts two weeks after cryoinjury. Transplanted ECs were incorporated into the new vessels, and increased regional perfusion in myocardial scar tissue, but failed to improve global function. Chekanov and colleagues [47] administered autologous ECs into the ischemic myocardium of sheep using a fibrin matrix, and demonstrated enhancement of neovascularization with improved left ventricular function. In tumor angiogenesis models [48, 49], implanted mature ECs similarly contributed to host neovascularization and tumor growth; furthermore genetic modification of the ECs with the anti-apoptotic gene Bcl-2 enhanced the

effects of cell implantation. These findings suggest that mature ECs have the potential to be incorporated into regenerating vessels *in vivo* under certain conditions.

The present results demonstrate that mature human ECs overexpressing the Id1 gene can be effectively incorporated into regenerating vessels in murine ischemic limbs. The extents of angiogenic and limb salvage effects were comparable to those of EPCs [37, 43, 44]. These results indicate that mature ECs could potentially be optimized for therapeutic angiogenesis by inducing phenotypic changes through appropriate gene transfers. Id1 gene transfer stimulated migration, proliferation, and tube formation of HUVECs *in vitro*, as previously shown in bovine aortic ECs [25] and HUVECs [50]. Migration and proliferation of ECs is considered a critical step for physiological as well as therapeutic angiogenesis [6, 43, 44]. In the present analysis, a part of transplanted SeV/Id1-HUVECs but not SeV/Null-HUVECs were in a proliferative state, indicating that stimulation of proliferation may contribute to the *in vivo* angiogenic effects of Id1. In addition, Id1 inhibited apoptosis of HUVECs under serum deprivation conditions. Id1 has been reported to both positively and negatively regulate apoptosis, depending on cell types and experimental conditions [40, 41, 50]. Sakurai et al. [50] have reported that overexpression of Id3, but not Id1, inhibits HUVEC apoptosis induced by serum starvation. The discrepancy between their results and ours may be explained by differences in culture condition and/or in Id1 expression levels. A previous study showed Id1 to delay the onset of replicative senescence in human ECs [51], Id1 may thereby increase the survival of SeV/Id1-HUVECs and contribute to angiogenesis.

In the present study, Id1 gene transfer upregulated the expression of Ang1 but not Ang2 in HUVECs. Furthermore, the present study revealed that upregulated Ang1 functionally contributed to the *in vitro* angiogenic effects of Id1 as an

autocrine/paracrine factor. Ang1 is reported to augment EC migration and protect ECs against apoptosis partly via the activation of Tie2/PI3-kinase/Akt signal transduction pathway [34, 52, 53]. Upregulation of the signaling pathway may partly explain the survival of SeV/Id1-HUVECs. However, in the previous studies [52, 54], it remains controversial whether Ang1 stimulates EC proliferation. Id1 is reported to inhibit Ets-1, a non-basic HLH protein, which promotes cell-cycle exit via indirectly promoting inactivation of the retinoblastoma protein by downregulating cyclin-dependent kinase inhibitors such as INK4a [55]. Ang1 upregulation, therefore, may contribute to the mechanism underlying the *in vivo* angiogenic effect of Id1-transfected HUVECs, together with other possible downstream targets such as metalloproteinases, integrins, fibroblast growth factor receptor, and INK4a genes, as suggested by previous studies using Id gene-deleted mice [21, 24], Id1-transfected ECs [50], and non-ECs [55].

It remains unknown whether the effect of Id1 on Ang1 expression is direct in the present study. Although regulation of Ang1 expression was not fully analyzed yet, a few reports [56, 57] have identified its regulatory transcriptional factors. AML-1 (CBF-α/CBFA2), a member of the runt transcriptional factor family, was shown to be one of the main factors regulating constitutive expression of Ang1 in murine hematopoietic cells by using a gain or loss of function study [57]. In fact, several AML-1-binding sequences are identified in the human Ang1 promoter region (within –3kb) as recently reported [56]. In addition, the ETS transcriptional factor ESE-1 has been identified as a functional mediator of Ang1 expression in the setting of inflammation [56]. To my best knowledge, however, there are no reports regarding the regulation of Ang1 by basic HLH transcriptional factors.

I analyzed endogenous Id1 expression levels with immunohistochemical technique in the tissue section of murine ischemic limbs. However, I could not detect significant upregulation of Id1 in ECs. In addition, DFX, an agent mimicking hypoxic condition, downregulated Id1 expression in cultured HUVECs although it caused VEGF upregulation, suggesting that Id1 expression is not induced in ischemic lesion. This result suggests that ischemia-induced suppression of Id1 expression may overcome the inductive effect of VEGF on Id1 expression. Therefore, Id1 gene transfer is expected to complement the downregulated activity of Id1 to confer angiogenic capacity on ECs.

In the present study, for gene transfer I used SeV vector, which has been shown to mediate higher levels of gene transfer in various organs than other vectors such as liposomes and adeno-associated virus [27, 58-60]. Briefly exposing organs to SeV-vector solution is enough for efficient gene transfer, after which expression of the viral genome, along with the exogenous gene, is relatively stable in both proliferating and arrested cells for at least 1 month *in vitro*. In addition, SeV's ability to mediate high levels of transfection and transgene expression independently of the cell cycle is a distinct advantage of this vector over adenoviral vectors. In the clinical setting, however, viral vectors including SeV vector may consider quite hard to use for gene transfer. Therefore, non-viral vector, characterized by highly efficient gene transfer and high and long-lasting transgene expression, is expected developed in the future.

Contrary to the beneficial angiogenic effect, it has been reported that the Id1 transgene may induce neoplastic transformation of ECs [19, 61]. In a previous study [51], however, Id1-transferred ECs were not immortalized and eventually underwent senescence despite high Id1 levels. In addition, no tumor formation was

pathologically observed in the lesions with transplanted SeV/Id1-HUVECs in our present study (data not shown). In addition, the *ex vivo* gene transfer strategy may preclude recipients from being exposed to the Id1 gene-bearing vector.

IV. Conclusion

Id1 gene transfer conferred mature vascular ECs with an angiogenic property, contributing to neovascularization after transplantation into ischemic lesions. The combination of Id1 gene transfer and transplantation using mature vascular ECs may serve as a novel and useful application for therapeutic revascularization with high efficiency and low risk.

V. References

1. Losordo, D.W. and Dimmeler, S.
Therapeutic angiogenesis and vasculogenesis for ischemic disease. Part I: angiogenic cytokines.
Circulation, 2004; 109(21): 2487-91.

2. Emanueli, C. and Madeddu, P.
Changing the logic of therapeutic angiogenesis for ischemic disease.
Trends Mol Med, 2005; 11(5): 207-16.

3. Simons, M. and Ware, J.A.
Therapeutic angiogenesis in cardiovascular disease.
Nat Rev Drug Discov, 2003; 2(11): 863-71.

4. Losordo, D.W. and Dimmeler, S.
Therapeutic angiogenesis and vasculogenesis for ischemic disease: part II: cell-based therapies.
Circulation, 2004; 109(22): 2692-7.

5. Carmeliet, P.
Mechanisms of angiogenesis and arteriogenesis.
Nat Med, 2000; 6(4): 389-95.

6. Risau, W.
Mechanisms of angiogenesis.
Nature, 1997; 386(6626): 671-4.

7. Asahara, T., Murohara, T., Sullivan, A., Silver, M., van der Zee, R., Li, T., Witzenbichler, B., Schatteman, G., and Isner, J.M.
Isolation of putative progenitor endothelial cells for angiogenesis.
Science, 1997; 275(5302): 964-7.

8. Shi, Q., Rafii, S., Wu, M.H., Wijelath, E.S., Yu, C., Ishida, A., Fujita, Y., Kothari, S., Mohle, R., Sauvage, L.R., Moore, M.A., Storb, R.F., and Hammond, W.P.
Evidence for circulating bone marrow-derived endothelial cells.
Blood, 1998; 92(2): 362-7.

9. Takahashi, T., Kalka, C., Masuda, H., Chen, D., Silver, M., Kearney, M., Magner, M., Isner, J.M., and Asahara, T.
Ischemia- and cytokine-induced mobilization of bone marrow-derived endothelial progenitor cells for neovascularization.
Nat Med, 1999; 5(4): 434-8.

10. Asahara, T., Masuda, H., Takahashi, T., Kalka, C., Pastore, C., Silver, M., Kearne, M., Magner, M., and Isner, J.M.
Bone marrow origin of endothelial progenitor cells responsible for postnatal vasculogenesis in physiological and pathological neovascularization.

Circ Res, 1999; 85(3): 221-8.

11. Rafii, S. and Lyden, D.
Therapeutic stem and progenitor cell transplantation for organ vascularization and regeneration.
Nat Med, 2003; 9(6): 702-12.

12. Balconi, G., Pietra, A., Busacca, M., de Gaetano, G., and Dejana, E.
Success rate of primary human endothelial cell culture from umbilical cords is influenced by maternal and fetal factors and interval from delivery.
In Vitro, 1983; 19(11): 807-10.

13. Gupta, K., Ramakrishnan, S., Browne, P.V., Solovey, A., and Hebbel, R.P.
A novel technique for culture of human dermal microvascular endothelial cells under either serum-free or serum-supplemented conditions: isolation by panning and stimulation with vascular endothelial growth factor.
Exp Cell Res, 1997; 230(2): 244-51.

14. Marchetti, S., Gimond, C., Iljin, K., Bourcier, C., Alitalo, K., Pouyssegur, J., and Pages, G.
Endothelial cells genetically selected from differentiating mouse embryonic stem cells incorporate at sites of neovascularization in vivo.
J Cell Sci, 2002; 115(Pt 10): 2075-85.

15. Reyes, M., Dudek, A., Jahagirdar, B., Koodie, L., Marker, P.H., and Verfaillie, C.M.
Origin of endothelial progenitors in human postnatal bone marrow.
J Clin Invest, 2002; 109(3): 337-46.

16. Kim, E.J., Li, R.K., Weisel, R.D., Mickle, D.A., Jia, Z.Q., Tomita, S., Sakai, T., and Yau, T.M.
Angiogenesis by endothelial cell transplantation.
J Thorac Cardiovasc Surg, 2001; 122(5): 963-71.

17. Norton, J.D., Deed, R.W., Craggs, G., and Sablitzky, F.
Id helix-loop-helix proteins in cell growth and differentiation.
Trends Cell Biol, 1998; 8(2): 58-65.

18. Massari, M.E. and Murre, C.
Helix-loop-helix proteins: regulators of transcription in eucaryotic organisms.
Mol Cell Biol, 2000; 20(2): 429-40.

19. Lasorella, A., Uo, T., and Iavarone, A.
Id proteins at the cross-road of development and cancer.
Oncogene, 2001; 20(58): 8326-33.

20. Zebedee, Z. and Hara, E.
Id proteins in cell cycle control and cellular senescence.
Oncogene, 2001; 20(58): 8317-25.

21. Lyden, D., Young, A.Z., Zagzag, D., Yan, W., Gerald, W., O'Reilly, R., Bader, B.L., Hynes, R.O., Zhuang, Y., Manova, K., and Benezra, R.
Id1 and Id3 are required for neurogenesis, angiogenesis and vascularization of tumour xenografts.
Nature, 1999; 401(6754): 670-7.

22. Lyden, D., Hattori, K., Dias, S., Costa, C., Blaikie, P., Butros, L., Chadburn, A., Heissig, B., Marks, W., Witte, L., Wu, Y., Hicklin, D., Zhu, Z., Hackett, N.R., Crystal, R.G., Moore, M.A., Hajjar, K.A., Manova, K., Benezra, R., and Rafii, S.
Impaired recruitment of bone-marrow-derived endothelial and hematopoietic precursor cells blocks tumor angiogenesis and growth.
Nat Med, 2001; 7(11): 1194-201.

23. de Candia, P., Solit, D.B., Giri, D., Brogi, E., Siegel, P.M., Olshen, A.B., Muller, W.J., Rosen, N., and Benezra, R.
Angiogenesis impairment in Id-deficient mice cooperates with an Hsp90 inhibitor to completely suppress HER2/neu-dependent breast tumors.
Proc Natl Acad Sci U S A, 2003; 100(21): 12337-42.

24. Ruzinova, M.B., Schoer, R.A., Gerald, W., Egan, J.E., Pandolfi, P.P., Rafii, S., Manova, K., Mittal, V., and Benezra, R.
Effect of angiogenesis inhibition by Id loss and the contribution of bone-marrow-derived endothelial cells in spontaneous murine tumors.
Cancer Cell, 2003; 4(4): 277-89.

25. Valdimarsdottir, G., Goumans, M.J., Rosendahl, A., Brugman, M., Itoh, S., Lebrin, F., Sideras, P., and ten Dijke, P.
Stimulation of Id1 expression by bone morphogenetic protein is sufficient and necessary for bone morphogenetic protein-induced activation of endothelial cells.
Circulation, 2002; 106(17): 2263-70.

26. Kato, A., Sakai, Y., Shioda, T., Kondo, T., Nakanishi, M., and Nagai, Y.
Initiation of Sendai virus multiplication from transfected cDNA or RNA with negative or positive sense.
Genes Cells, 1996; 1(6): 569-79.

27. Kato, A., Kiyotani, K., Hasan, M.K., Shioda, T., Sakai, Y., Yoshida, T., and Nagai, Y.
Sendai virus gene start signals are not equivalent in reinitiation capacity: moderation at the fusion protein gene.
J Virol, 1999; 73(11): 9237-46.

28. Kang, H.J., Kim, S.C., Kim, Y.J., Kim, C.W., Kim, J.G., Ahn, H.S., Park, S.I., Jung, M.H., Choi, B.C., and Kimm, K.
Short-term phytohaemagglutinin-activated mononuclear cells induce endothelial progenitor cells from cord blood CD34+ cells.
Br J Haematol, 2001; 113(4): 962-9.

29. Currie, M.J., Gunningham, S.P., Turner, K., Han, C., Scott, P.A., Robinson, B.A., Chong, W., Harris, A.L., and Fox, S.B.
Expression of the angiopoietins and their receptor Tie2 in human renal clear cell carcinomas; regulation by the von Hippel-Lindau gene and hypoxia.
J Pathol, 2002; 198(4): 502-10.

30. Krussel, J.S., Casan, E.M., Raga, F., Hirchenhain, J., Wen, Y., Huang, H.Y., Bielfeld, P., and Polan, M.L.
Expression of mRNA for vascular endothelial growth factor transmembraneous receptors Flt1 and KDR, and the soluble receptor sflt in cycling human endometrium.
Mol Hum Reprod, 1999; 5(5): 452-8.

31. Scicchitano, M.S., McFarland, D.C., Tierney, L.A., Narayanan, P.K., and Schwartz, L.W.
In vitro expansion of human cord blood CD36+ erythroid progenitors: temporal changes in gene and protein expression.
Exp Hematol, 2003; 31(9): 760-9.

32. Huang, J., Hardy, J.D., Sun, Y., and Shively, J.E., *Essential role of biliary glycoprotein (CD66a) in morphogenesis of the human mammary epithelial cell line MCF10F.* J Cell Sci, 1999; 112 (Pt 23): 4193-4205.

33. Tamura, M., Gu, J., Matsumoto, K., Aota, S., Parsons, R., and Yamada, K.M., *Inhibition of cell migration, spreading, and focal adhesions by tumor suppressor PTEN.* Science, 1998; 280(5369): 1614-1617.

34. Kwak, H.J., So, J.N., Lee, S.J., Kim, I., and Koh, G.Y., *Angiopoietin-1 is an apoptosis survival factor for endothelial cells.* FEBS Lett, 1999; 448(2-3): 249-253.

35. Karawajew, L., Ruppert, V., Wuchter, C., Kosser, A., Schrappe, M., Dorken, B., and Ludwig, W.D., *Inhibition of in vitro spontaneous apoptosis by IL-7 correlates with bcl-2 up-regulation, cortical/mature immunophenotype, and better early cytoreduction of childhood T-cell acute lymphoblastic leukemia.*
Blood, 2000; 96(1): 297-306.

36. Couffinhal, T., Silver, M., Zheng, L.P., Kearney, M., Witzenbichler, B., and Isner, J.M.
Mouse model of angiogenesis.
Am J Pathol, 1998; 152(6): 1667-79.

37. Kalka, C., Masuda, H., Takahashi, T., Kalka-Moll, W.M., Silver, M., Kearney, M., Li, T., Isner, J.M., and Asahara, T.
Transplantation of ex vivo expanded endothelial progenitor cells for therapeutic neovascularization.
Proc Natl Acad Sci U S A, 2000; 97(7): 3422-7.

38. Tournay, O. and Benezra, R.

Transcription of the dominant-negative helix-loop-helix protein Id1 is regulated by a protein complex containing the immediate-early response gene Egr-1.
Mol Cell Biol, 1996; 16(5): 2418-30.

39. Goumans, M.J., Valdimarsdottir, G., Itoh, S., Rosendahl, A., Sideras, P., and ten Dijke, P.
Balancing the activation state of the endothelium via two distinct TGF-beta type I receptors.
Embo J, 2002; 21(7): 1743-53.

40. Ling, M.T., Wang, X., Ouyang, X.S., Xu, K., Tsao, S.W., and Wong, Y.C.
Id-1 expression promotes cell survival through activation of NF-kappaB signalling pathway in prostate cancer cells.
Oncogene, 2003; 22(29): 4498-508.

41. Tanaka, K., Pracyk, J.B., Takeda, K., Yu, Z.X., Ferrans, V.J., Deshpande, S.S., Ozaki, M., Hwang, P.M., Lowenstein, C.J., Irani, K., and Finkel, T.
Expression of Id1 results in apoptosis of cardiac myocytes through a redox-dependent mechanism.
J Biol Chem, 1998; 273(40): 25922-8.

42. Teichert-Kuliszewska, K., Maisonpierre, P.C., Jones, N., Campbell, A.I., Master, Z., Bendeck, M.P., Alitalo, K., Dumont, D.J., Yancopoulos, G.D., and Stewart, D.J.
Biological action of angiopoietin-2 in a fibrin matrix model of angiogenesis is associated with activation of Tie2.
Cardiovasc Res, 2001; 49(3): 659-70.

43. Iwaguro, H., Yamaguchi, J., Kalka, C., Murasawa, S., Masuda, H., Hayashi, S., Silver, M., Li, T., Isner, J.M., and Asahara, T.
Endothelial progenitor cell vascular endothelial growth factor gene transfer for vascular regeneration.
Circulation, 2002; 105(6): 732-8.

44. Murasawa, S., Llevadot, J., Silver, M., Isner, J.M., Losordo, D.W., and Asahara, T.
Constitutive human telomerase reverse transcriptase expression enhances regenerative properties of endothelial progenitor cells.
Circulation, 2002; 106(9): 1133-9.

45. Murohara, T., Ikeda, H., Duan, J., Shintani, S., Sasaki, K., Eguchi, H., Onitsuka, I., Matsui, K., and Imaizumi, T.
Transplanted cord blood-derived endothelial precursor cells augment postnatal neovascularization.
J Clin Invest, 2000; 105(11): 1527-36.

46. Shintani, S., Murohara, T., Ikeda, H., Ueno, T., Sasaki, K., Duan, J., and Imaizumi, T.

Augmentation of postnatal neovascularization with autologous bone marrow transplantation.
Circulation, 2001; 103(6): 897-903.

47. Chekanov, V., Akhtar, M., Tchekanov, G., Dangas, G., Shehzad, M.Z., Tio, F., Adamian, M., Colombo, A., Roubin, G., Leon, M.B., Moses, J.W., and Kipshidze, N.N.
Transplantation of autologous endothelial cells induces angiogenesis.
Pacing Clin Electrophysiol, 2003; 26(1 Pt 2): 496-9.

48. Nor, J.E., Christensen, J., Liu, J., Peters, M., Mooney, D.J., Strieter, R.M., and Polverini, P.J.
Up-Regulation of Bcl-2 in microvascular endothelial cells enhances intratumoral angiogenesis and accelerates tumor growth.
Cancer Res, 2001; 61(5): 2183-8.

49. Koizumi, K., Tsutsumi, Y., Kamada, H., Yoshioka, Y., Watanabe, M., Yamamoto, Y., Okamoto, T., Mukai, Y., Nakagawa, S., Tani, Y., and Mayumi, T.
Incorporation of adult organ-derived endothelial cells into tumor blood vessel.
Biochem Biophys Res Commun, 2003; 306(1): 219-24.

50. Sakurai, D., Tsuchiya, N., Yamaguchi, A., Okaji, Y., Tsuno, N.H., Kobata, T., Takahashi, K., and Tokunaga, K.
Crucial role of inhibitor of DNA binding/differentiation in the vascular endothelial growth factor-induced activation and angiogenic processes of human endothelial cells.
J Immunol, 2004; 173(9): 5801-9.

51. Tang, J., Gordon, G.M., Nickoloff, B.J., and Foreman, K.E.
The helix-loop-helix protein id-1 delays onset of replicative senescence in human endothelial cells.
Lab Invest, 2002; 82(8): 1073-9.

52. Witzenbichler, B., Maisonpierre, P.C., Jones, P., Yancopoulos, G.D., and Isner, J.M.
Chemotactic properties of angiopoietin-1 and -2, ligands for the endothelial-specific receptor tyrosine kinase Tie2.
J Biol Chem, 1998; 273(29): 18514-21.

53. Kim, I., Kim, H.G., So, J.N., Kim, J.H., Kwak, H.J., and Koh, G.Y.
Angiopoietin-1 regulates endothelial cell survival through the phosphatidylinositol 3'-Kinase/Akt signal transduction pathway.
Circ Res, 2000; 86(1): 24-29.

54. Kanda, S., Miyata, Y., Mochizuki, Y., Matsuyama, T., and Kanetake, H.
Angiopoietin 1 is mitogenic for cultured endothelial cells.
Cancer Res, 2005; 65(15): 6820-7.

55. Ohtani, N., Zebedee, Z., Huot, T.J., Stinson, J.A., Sugimoto, M., Ohashi, Y., Sharrocks, A.D., Peters, G., and Hara, E.
Opposing effects of Ets and Id proteins on p16INK4a expression during cellular senescence.
Nature, 2001; 409(6823): 1067-70.

56. Brown, C., Gaspar, J., Pettit, A., Lee, R., Gu, X., Wang, H., Manning, C., Voland, C., Goldring, S.R., Goldring, M.B., Libermann, T.A. Gravallese, E.M., and Oettgen, P., *ESE-1 is a novel transcriptional mediator of angiopoietin-1 expression in the setting of inflammation.*
J Biol Chem, 2004; 279(13): 12794-803.

57. Takakura, N., Watanabe, T., Suenobu, S., Yamada, Y., Noda, T., Ito, Y., Satake, M., and Suda, T.
A role for hematopoietic stem cells in promoting angiogenesis.
Cell, 2000; 102(2): 199-209.

58. Hasan, M.K., Kato, A., Shioda, T., Sakai, Y., Yu, D., and Nagai, Y.
Creation of an infectious recombinant Sendai virus expressing the firefly luciferase gene from the 3' proximal first locus.
J Gen Virol, 1997; 78 (Pt 11): 2813-20.

59. Yonemitsu, Y., Kitson, C., Ferrari, S., Farley, R., Griesenbach, U., Judd, D., Steel, R., Scheid, P., Zhu, J., Jeffery, P.K., Kato, A., Hasan, M.K., Nagai, Y., Masaki, I., Fukumura, M., Hasegawa, M., Geddes, D.M., and Alton, E.W.
Efficient gene transfer to airway epithelium using recombinant Sendai virus.
Nat Biotechnol, 2000; 18(9): 970-3.

60. Masaki, I., Yonemitsu, Y., Komori, K., Ueno, H., Nakashima, Y., Nakagawa, K., Fukumura, M., Kato, A., Hasan, M.K., Nagai, Y., Sugimachi, K., Hasegawa, M., and Sueishi, K.
Recombinant Sendai virus-mediated gene transfer to vasculature: a new class of efficient gene transfer vector to the vascular system.
Faseb J, 2001; 15(7): 1294-6.

61. Alani, R.M., Hasskarl, J., Grace, M., Hernandez, M.C., Israel, M.A., and Munger, K.
Immortalization of primary human keratinocytes by the helix-loop-helix protein, Id-1.
Proc Natl Acad Sci U S A, 1999; 96(17): 9637-41.